

SHRP-A-699

# Performance Prediction Models In the Superpave Mix Design System

Harold L. Von Quintus  
Brent Rauhut Engineering Inc.



**Strategic Highway Research Program**  
National Research Council  
Washington, DC 1994

SHRP-A-699  
Contract A-005  
Product no. 1012

Program Manager: *Edward T. Harrigan*  
Project Manager: *Harold L. Von Quintus*  
Program Area Secretary: *Juliet Narsiah*

August 1994

key words:  
accelerated performance tests  
constitutive relationships  
mix design method  
pavement performance, modeling of  
performance prediction model  
response model  
Superpave

Strategic Highway Research Program  
National Research Council  
2101 Constitution Avenue N.W.  
Washington, DC 20418

(202) 334-3774

The publication of this report does not necessarily indicate approval or endorsement by the National Academy of Sciences, the United States Government, or the American Association of State Highway and Transportation Officials or its member states of the findings, opinions, conclusions, or recommendations either inferred or specifically expressed herein.

©1994 National Academy of Sciences

## **Acknowledgments**

The research described herein was supported by the Strategic Highway Research Program (SHRP). SHRP is a unit of the National Research Council that was authorized by section 128 of the Surface Transportation and Uniform Relocation Assistance Act of 1987.

# Contents

1	Introduction	1
2	Factors Considered in Developing the Pavement Performance Prediction Models	3
3	Material Property Relationships—The Constitutive Equations	9
	3.1 Elastic Properties: A Non-Linear Elasticity Model	11
	3.1.1 Resilient Modulus	12
	3.1.2 Poisson’s Ratio	13
	3.2 Time-Dependency Properties: The Viscoelastic Model	17
	3.2.1 Load-Related Response Model	17
	3.2.2 Non-Load Related Response Model	20
	3.3 Inelastic Properties: The Plasticity Model	21
	3.3.1 Elastoplasticity Formulation	22
	3.3.2 The Vermeer Model	24
	3.4 Fracture Properties: The Strength Model	29
4	The Pavement Response Model	31
	4.1 Finite Element Program	31
	4.2 The Incremental Stress-Strain Relation	31
5	Thermal Cracking Model Formulation	37
	5.1 Calculation of Thermal Stresses	37
	5.2 Pavement Distress Model	39
	5.2.1 Stress Intensity Factor Model	39
	5.2.2 Crack Depth (Fracture) Model	39
	5.2.3 Crack Amount Model	41
6	Fatigue Cracking Model Formulation	43
	6.1 Fatigue Mechanisms	43
	6.2 Cumulative Damage Theory	44
	6.3 Modelling Approach	45
	6.3.1 Regression Equations	45
	6.3.2 Fracture Mechanics	45
	6.4 Fatigue Cracking Model	47
	6.4.1 Crack Initiation	47

	6.4.2 Healing . . . . .	49
	6.4.3 Crack Propagation . . . . .	50
	6.4.4 Cracking Amount . . . . .	52
7	Rutting Model Formulation . . . . .	53
	7.1 Permanent Deformation Characterization . . . . .	54
	7.2 Calculation of Rut Depth . . . . .	55
8	Accelerated Laboratory Tests For Performance Predictions . . . . .	59
	8.1 Analysis of Test Results . . . . .	59
9	Pavement performance prediction model . . . . .	67
	9.1 Aging Considerations . . . . .	67
	9.2 Non-Load Related Performance Model . . . . .	67
	9.2.1 Inputs Module . . . . .	68
	9.3 Laboratory Tensile Tests and the Transformation Model . . . . .	72
	9.3.1 Tensile Tests at Low Temperatures . . . . .	72
	9.3.2 Transformation Model . . . . .	72
	9.4 Load-Related Performance Models . . . . .	79

## List of Figures

Figure 3.1	Response Components from the Creep-Recovery Test of a Viscoelastic-Plastic Material . . . . .	10
Figure 3.2	Comparison of Predictions and Observations for Shear Test Using the $k_1$ - $k_5$ model on asphalt concrete . . . . .	14
Figure 4.1	Comparison of Predictions and Observations for Uniaxial Strain Test Using the $k_1$ - $k_5$ model on asphalt concrete . . . . .	34
Figure 4.2	Comparison of Predictions and Observations for Volumetric Compression Test Using the $k_1$ - $k_5$ model on asphalt concrete . . . . .	35
Figure 4.3	Comparison of Predictions and Observations for Shear Test Using the $k_1$ - $k_5$ model on asphalt concrete . . . . .	36
Figure 8.1	Loading and Unloading Scheme Used in the Volumetric, Uniaxial Strain, and Constant-Height Simple Shear Tests . . . . .	62
Figure 8.2	Example of the Applied Loading (Confining Pressure) and Response Output (Vertical Strain) with Time from the Volumetric Test . . . . .	63
Figure 8.3	Example of the Applied Loading (Axial Load or Vertical Pressure) and Response Output (Vertical Deformation or Strain) with Time from the Uniaxial Strain Test . . . . .	64
Figure 8.4	Example of the Applied Loading (Shear Stress or Lateral Load) and Response Output (Shear Strain or Horizontal Deformation) with Time from the Constant-Height Simple Shear Test . . . . .	65
Figure 9.1	Major Components of the Low Temperature Cracking Model . . . . .	69
Figure 9.2	Detailed Schematic of the Low Temperature Cracking Model . . . . .	70
Figure 9.3	Creep Compliance Curves for PTI Section 23 . . . . .	73
Figure 9.4	Master Creep Compliance Curve for PTI Section 23 . . . . .	76
Figure 9.5	Shift Factor versus Temperature for PTI Section 23 . . . . .	77
Figure 9.6	Master Relaxation Modulus Curve for PTI Section 23 . . . . .	80

## Abstract

The objectives of SHRP's asphalt research program were: to extend the life or reduce the life-cycle costs of asphalt pavements; to reduce maintenance costs; and to minimize the number of premature pavement failures. An important result of this research effort is the development of performance-based asphalt binder and asphalt paving mix specifications to control three distress modes: permanent deformation; fatigue cracking; and low-temperature cracking.

The SHRP-005 contract developed detailed pavement performance models to support the development of these specifications, and as an integral tool for mix design in the Superpave mix design system. This report summarizes the theoretical development, structure, and features of these performance models.

Comprehensive pavement performance models were developed that predict the amount of permanent deformation and fatigue cracking (the load-related model) and the amount of low-temperature cracking (the non-load-related model) developed over time in asphalt concrete pavements constructed with paving mixes designed with the Superpave system or other mix design methods. The models employ test results from the Superpave accelerated performance tests combined with detailed environmental, structural, and traffic data to determine the optimal mix design for the given conditions, or to analyze the potential performance of field cores.

The models are relatively uncomplicated, and run on 80486 or similar microcomputers under the control of the *Superpave Specification, Design, and Support Software* with which they are packaged. The models can minimize a specific distress or combinations of different distresses, or they can set specification limits for specific materials and environments.

# 1

## Introduction

SHRP research contract A-005 was responsible for developing performance prediction models for both asphalt binders and asphalt paving mixes. The purpose of this report is to describe the development and integration of: the constitutive equations used to describe the mixture behavior; the pavement response model; the use of the accelerated performance tests to measure critical material properties; and the integration of all these components into the pavement performance prediction models incorporated into the Superpave mix design system. A detailed description on the development and validation of the pavement performance prediction models is included in the final report on the SHRP A-005 contract (Lytton, Uzan and others, 1993).

This report first provides a discussion on the different assumptions included in the chosen approach, including the type of analysis (static as compared to dynamic loads), the type of material properties required (nonlinear elastic as compared to nonlinear elasto-visco-plastic material), etc. This is followed by a description of the models chosen for predicting pavement performance. The calibration process for correcting the deviations of the predictions due to the effects of the various assumptions described herein are discussed in detail by Lytton, Uzan and others (1993).



## Factors Considered in Developing the Pavement Performance Prediction Models

The factors entering into the prediction of pavement performance are numerous and complex. They include loading, environmental, construction and material property variables which interact with one another. It was beyond the scope of the SHRP A-005 contract to develop a model that includes directly all these variables. Instead, a simplified approach based on the quasi-nonlinear elastic approximation was adopted. Thus, it is important to recognize that the development of models under the SHRP A-005 contract was guided by the following ground rules:

- Develop computer software suitable for use on personal computer systems based on the 80486 microprocessor.
- Improve the estimation of the states of stress and strain in the primary response model.
- Incorporate a mechanistic approach in the distress prediction modeling.
- Allow flexibility for replacing/improving selected or individual modules incorporated into the pavement performance prediction model or Superpave mix design system.
- Simplify whenever possible, but without sacrificing accuracy.

In addition to the above considerations, it should be recognized and understood that the performance of an asphalt concrete mixture is dependent upon the properties and configuration of the entire pavement structure or system. Thus, the stresses and strains in the asphalt concrete layer are a function of the underlying support and environment. But first, it is imperative to understand the effects of the variables and test procedures in order to be able to include them in the simplified approach. To begin with, some statements and discussions

are required about the initial development of the integrated models used to predict pavement distress as related to the behavior of pavement materials.

1. *Because of the non-linear elasto-visco-plastic behavior of pavement materials, the response of the pavement system in terms of induced stresses, strains and displacements is not symmetric with respect to the axle or wheel load position, ahead of and behind the load.* A shear stress reversal (opposite sign) takes place when a wheel approaches a given location and after it leaves it. Each infinitesimal element in the pavement would have a different stress-strain time history. In order to realistically simulate these conditions, it is necessary to analyze a dual wheel rolling on a 3-D (three dimensional) pavement structure with nonlinear elasto-visco-plastic models for asphalt concrete and clay materials, and nonlinear elasto-plastic models for granular materials. A time-marching scheme is needed for this case. (An analysis scheme of this kind is being developed for the Federal Aviation Administration as the *Unified Methodology for Airport Pavement Analysis and Design* with planned availability within the next decade. The present generation of pavement design is based on the quasi-static load with nonlinear materials).

2. *The rate of accumulation of the permanent deformation changes with the number of load repetitions.* For elasto-plastic materials, this behavior means that the kinematic hardening theory (in addition to the isotropic hardening one) must be used in the material modeling. In order to realistically simulate this condition, it is necessary to analyze each load repetition in its sequential order. For nonlinear elasto-visco-plastic materials, a complete material characterization and a definition of the loading-unloading states are required. With these loading-unloading states, a time-marching analysis scheme is necessary to simulate the load repetitions.

This type of analysis scheme requires a prohibitive amount of computer time and is not practical. Given the requirements noted above, simplified approaches must be formulated, checked and calibrated. However, the simplified approach should take into account the effects of traffic composition (mixed traffic consideration) and temporal variation of the pavement structure during the year and the analysis period. A simplified approach based on the "time hardening" scheme was adopted in the prediction of pavement rutting in the SHRP A-005 contract.

3. *Pavement materials (including the top of the subgrade in the case of an excavated cross section) are usually compacted to a high degree.* The purpose of the compaction is twofold: (a) to increase the strength of the material and (b) to increase its resistance to permanent deformation. In well constructed pavements, densification (permanent volume change due to isotropic stress changes) is usually very small compared to the shear deformation. In most cases, the volumetric component of the plastic flow can be neglected, thus avoiding numerical difficulties in the case of a double yielding surface and reducing the number of variables to a minimum.

4. *Pavement material compaction induces residual stresses which in turn affects the*

*pavement response and performance.* Although these types of residual stresses are not measured, their existence has been postulated on theoretical grounds (Uzan and others, 1992; Duncan and Seed, 1986; Seed and Duncan, 1986). It has been suggested that residual stresses of the order of 14-28 kPa are induced by the compaction process in the base and subbase materials. Since the residual stresses depend on the compaction and overburden loads on one hand and on the failure envelop on the other, it may be assumed that these residual stresses will not vary significantly during the analysis period. One may argue that the residual stresses induced by compaction will relax with time. However, they can be re-induced by heavy traffic loads. Thus it is unclear what the initial state of stress is before each load application, complicating the process of estimating the correct stress-strain state in the pavement structure.

5. *In the first load repetition, the permanent strain is relatively large compared to the elastic strain.* In elasto-plastic analyses, this may cause a stress and strain distribution that is different from the elastic analysis. However, after a few hundreds of load repetitions, the irrecoverable component of strain is very small compared to the elastic or total strain. The state of stress and deformation is only slightly dependent on the plastic strain. The final state of stress under the n-th load repetition depends mainly on the initial state of stress and the elastic component of the stress-strain constitutive law. Therefore, an elastic analysis (neglecting the small plastic component) is considered adequate for estimating the stresses and strains induced by the load (in addition to the initial state of stress and strain in an accumulated state due to all previous load and unload cycles). It can be estimated by simulating every load in sequence and taking into account relaxation or healing due to temperature changes in the bituminous layer. As stated before, such an analysis is impractical because of the computer time required.

6. *Temperature variation in the asphalt concrete layer during the day, year and analysis period has a significant effect on the stresses and strains that occur in the mixture from some applied load. The development of this stress-state has a direct impact on the occurrence of both the load and non-load related distresses.* In the cooling process, tensile stresses develop which may cause thermal cracking. Any previously induced compressive stresses are relaxed in the cooling process. Thermal cracking usually occurs at very low temperatures, (usually below -10°C). Conversely, in the heating process, compressive stresses may develop. Due to the elasto-visco-plastic nature of the bituminous material and the long time associated with the temperature variation, however, these compressive stresses will be relatively small at high temperatures. Also, any induced stresses in the bituminous layer due to compaction, or plastic flow caused by traffic, will relax with time.

In summary, a realistic analysis of the stresses and strains in a pavement structure due to load and environmental changes is very complex. At present, it is not practical to use such an approach because it is prohibitively (computer) time consuming, and, most importantly, several mechanisms of stress induction and relaxation are not fully understood.

Thus, the SHRP A-005 contractor hypothesized that:

- The initial state of stress before every load repetition is affected by both the previous load repetitions and the environmental conditions (as they vary with time). Only small residual stresses are assumed to exist in both asphalt concrete and granular materials.
- After several hundreds of load repetitions, a quasi-nonlinear elastic analysis may be adequate for estimating the state of the stress and strain from the applied load.

As a result, the primary response model used in Superpave mix design system software is based on quasi-static nonlinear elastic analysis. The moving wheel and its dynamic effects are not simulated. The traffic load is represented by a dual-wheel of the standard 80 kN axle load. A theoretical contradiction was found between nonlinear elastic analysis using 2-D (two-dimensional) FE (finite element) programs and the dual-wheel type of loading. The dual wheel type cannot be represented in the 2-D axisymmetric conditions. Each wheel can be separately represented in the 2-D axisymmetric conditions. The nonlinear analysis does not allow one to use load superposition, as superposition can be considered only for linear systems.

The nonlinear elastic material characterization has been proven to be very efficient in improving the computed states of stress in pavements (Uzan and others, 1990). Because of dilation effects that are noticeable at large principal stress ratios, compressive stresses are computed in the granular base and subbase materials. This is an appreciable improvement over the linear elastic analyses where tensile stresses are computed at the bottom of the granular base and subbase layers. In the current version of the Superpave performance prediction software, the distress models are separated or uncoupled from the primary response model for the following reasons and considerations:

- *It is impractical to run the primary response model (FE program) for each load application.*
- *After several hundreds of load repetitions, the permanent or inelastic component of the deformation is very small compared to the elastic one, and the initial state of stress before the application of the n-th load repetition is difficult to estimate, as discussed above. Thus, state of stress under the n-th load is dictated by the elastic nonlinear behavior of the material.*
- *The elasto-plasticity theory for the first load repetition was used for estimating the state of stress and strain (elastic and plastic). Specifically, the Vermeer non-associative plasticity model was used to characterize the pavement materials.*

It was found that the elasto-plastic model becomes unstable for materials with friction angles in excess of 50 degrees. Since granular base and subbase materials exhibit large

friction angles of 60 degrees and higher, the use of the elasto-plasticity model was abandoned for these granular materials, and quasi-nonlinear elastic analysis was adopted for estimating the state of stress (which corresponds to the anticipated one after a few hundred load repetitions). However, if a solution to the instability can be found, the nonlinear elastic analysis may be replaced by an elasto-plastic one.

- *Because of the assumptions made in the development of the Superpave performance models, adjustments, termed calibration factors, must be applied to account for any resulting inaccuracies in the models.*

This process is called "calibration" and involves the analysis of multiple field pavement sections. In the case of "coupling" between the primary response and the distress models, both programs must be run every time a parameter is changed. In the case of "uncoupling" between these programs, only the distress model must be rerun when a parameter is changed. Due to its relative simplicity, the uncoupled procedure was employed in the A-005 model development.

In summary, the following assumptions were incorporated in the models:

1. Loading Assumptions

- static weight of 80 Kn single axle
- only vertical loads are considered
- circular loading area for each wheel load
- dual wheel load of the standard 80 kn single axle
- load repetitions corresponding to 0.1 seconds loading and 0.9 seconds unloading
- uniform traffic with one single axle load type
- no traffic wander

2. Environmental Assumptions

- The temperature, moisture (suction) and freeze-thaw regime are constant within each season.
- Every year is subdivided into n-seasons with different layers of different material properties. Each season is at least one month long. Average moduli and other parameters are used to represent the materials during each season.
- The monthly average temperature in the asphalt concrete layer, at a depth of one third the thickness of that layer is used to represent the temperature in the bituminous layer.
- Monthly moduli of the base, subbase and subgrade layers are used to represent the layers.

### 3

## Material Property Relationships - The Constitutive Equations

An important step in pavement performance analysis is the selection of a suitable constitutive equation to model the behavior of a mix under some external load. The constitutive or stress-strain law of engineering materials plays a significant role in providing reliable solutions to engineering problems. Unfortunately, a linear elastic model cannot adequately model the behavior of pavement materials. There are numerous non-linear constitutive models which have been developed in the last decade. For most typical pavement materials, the unloading material response follows a completely different path from that of loading in the inelastic range. When unloading to the initial state of stress takes place, the strains are not recovered completely and some permanent strains remain. Therefore, in order for the elastic-based model to be used under general stress histories, they must be accompanied by special arrangements to account for the unloading behavior.

A mixture's response to an applied load is assumed to be visco-elasto-plastic and is broken down into four basic components of deformation or strain. These are:

1. Elastic deformation which is recoverable and time independent.
2. Plastic deformation which is non recoverable and time independent.
3. Visco-elastic deformation which is recoverable and time dependent.
4. Visco-plastic deformation which is non recoverable and time dependent.

The creep/recovery test has been used for characterizing these four types of deformation. By applying a step load function for a *loading* period of time and unloading that stepped function for an *unloading* period of time, each of the mix responses can be identified. These responses are shown in Figure 3.1 and defined as:

- The instantaneous response measured during the unloading phase represents the elastic component of deformation ( $\epsilon_e$ ).
- The instantaneous response measured during the loading phase represents the elastic ( $\epsilon_e$ ) and plastic ( $\epsilon_p$ ) components of deformation. Subtracting the elastic component from the total deformation results in the plastic component of deformation.

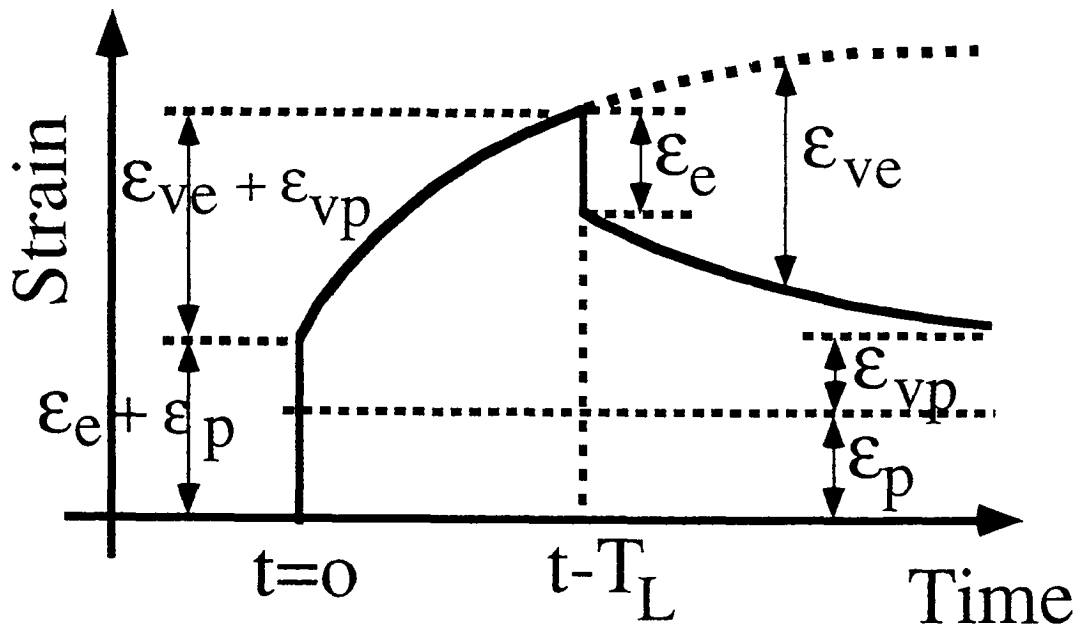
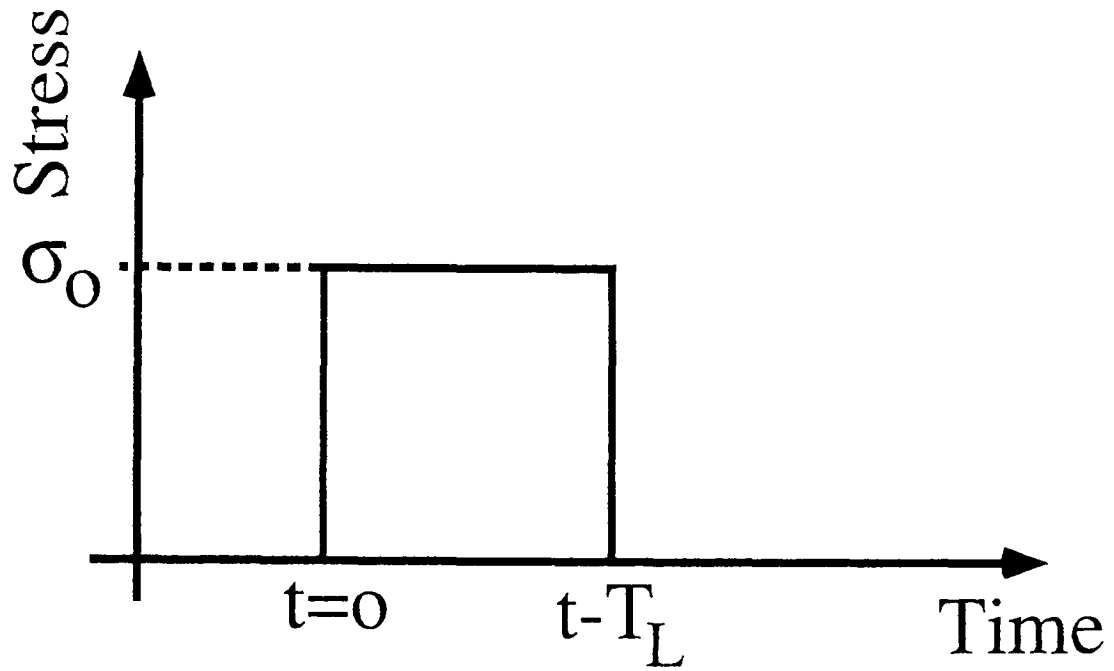


Figure 3.1. Response Components from the Creep-Recovery Test of a Viscoelastic-Plastic Material

- The visco-elastic and visco-plastic components, however, are more difficult to separate. The delayed response in the unloading phase is composed of only the visco-elastic response ( $\epsilon_{ve}$ ), whereas, the delayed response in the loading phase is composed of both the visco-elastic and visco-plastic response ( $\epsilon_{ve} + \epsilon_{vp}$ ). Assuming that the asphalt paving mix's response to load is visco-elasto-plastic, both the resilient and permanent deformation can be estimated for different loading and unloading times by performing creep/recovery tests in both tension and compression. By performing creep/recovery tests at different stress conditions (with and without confinement) and temperatures, each of the material coefficients can be determined.

A materials evaluation model was initially developed by the SHRP A-005 contractor to determine the response of each of these components to an applied load and to calculate material properties. However, the computational time required for wheel loads with varying speeds and axle configurations is very time consuming and not applicable for day-to-day mix designs using presently available microcomputers. More specifically, the magnitude of each response component varies with temperature. At low temperatures, asphalt concrete primarily follows the principles of a linear visco-elastic material, but the higher the temperature the more important and significant are the response components which describe the viscoelastic and viscoplastic components.

Originally, it was suggested that one constitutive law be used with all temperatures and types of load (environmental and traffic induced). To maintain those requirements noted at the beginning of the chapter, however, simplicity and reduction of computational time were factors in selecting different constitutive equations describing the material behavior at different temperatures and loading types. As a result, models for the load (traffic) and non-load (environmental) related distresses were kept separate, or uncoupled.

To estimate the material coefficients and properties from the accelerated laboratory tests, a linear viscoelastic formulation was adopted by the A-005 contractor for the non-load related distress model, but an elasto-plasticity formulation was used within the load related pavement performance models. For the load related models, it is assumed that specimen deformation is composed of two parts; an elastic and plastic component or the recoverable and non-recoverable parts, respectively. An important part of the elasto-plastic approach is the failure law. This law constitutes an upper limit of the yield function and determines the shapes of the yield function and plastic potential.

### **3.1 Elastic Properties: A Non-Linear Elasticity Model**

The stress-strain behavior of pavement materials is very complicated and numerous factors affect the materials response to load. It has been shown that the characteristics such as nonlinearity, stress-path dependency, shear dilatancy, the effect of hydrostatic stress components, influence of intermediate principle stress, and the stress-induced anisotropy are very important features for a realistic representation of pavement materials. Such behavior is far too complicated to offer a simple yet realistic constitutive relation which is capable of



describing the behavior of materials under general loading conditions. Therefore, simplifying assumptions are often employed in the formulation of the constitutive model in practical applications by including a limited number of behavior characteristics that are relevant or critical to a particular problem. These are discussed in the following sections.

### 3.1.1 Resilient Modulus.

The concept of the resilient modulus is often used to characterize pavement materials. The resilient modulus refers to the unloading modulus during a triaxial test in which loading, unloading and reloading are simulated under static or cyclic loading conditions. A resilient modulus is defined as the ratio of the repeated deviatoric stress to the recoverable part of the axial strain. In this approach, the constitutive equations are developed directly as a simple modification of the isotropic linear relation (generalized Hooke's Law) with the elastic constants replaced by scalar functions associated with the stress. For this approach, a scalar function associated with the state of stress may be expressed in terms of the stress and variance.

In the resilient modulus model, any scalar function of stress can be used for the isotropic nonlinear elastic modulus. The constitutive models formulated on this basis are the Cauchy elastic type; the state of strain is determined uniquely by the current state of stress. However, this does not imply that strain energy density,  $W$ , calculated from such stress-strain relations is path independent. Certain restrictions must be imposed on the chosen scalar function in order to ensure the path-independent characteristics of  $W$ . This assures that the laws of thermodynamics are always satisfied and that energy is not generated during any loading-unloading cycle.

The modulus of elasticity or resilient modulus ( $E_R$ ) is defined by the following equation:

$$E_R = k_1 P_a \left( \frac{\theta + k_6}{P_a} \right)^{k_2} \left( \frac{\tau_{oct}}{P_a} \right)^{k_3} \quad (3.1)$$

where:  $k_1, k_2, k_3$  and  $k_6$  are material properties or constants and determined by regression analyses from the results of the accelerated laboratory tests.

$\theta$  =  $I_1 =$  first stress invariant ( $\sigma_1 + \sigma_2 + \sigma_3$ )  
 $\tau_{oct}$  = octahedral shear stress  
 $P_a$  = atmospheric pressure

This constitutive equation assumes an isotropic material, which of course is an incorrect assumption, but has long been used to simplify the mathematical treatment.

Equation 3.1 can be used as a "universal material model" for both granular and fine-

grained materials (Witczak and Uzan, 1988). It has the capability of representing a modulus decrease as the octahedral shear stress increases and a modulus increase as the first stress invariant ( $\theta$ ) increases. The equation can also be used to represent the so-called "stiffening effect" observed in the laboratory as an increase in the resilient modulus, as both the first stress invariant and octahedral shear stress increase at large deviatoric stresses (or large octahedral shear stresses). This stiffening effect is a characteristic of granular materials or aggregate in a dense packing condition, and is related to the dilation phenomenon.

In the resilient model (equation 3.1), the state of stress should be the effective stress, as identified below.

$$\sigma_{ij} = \sigma_{ij}^t - u\delta_{ij} \quad (3.2)$$

where:

$\sigma_{ij}$	=	effective stress
$\sigma_{ij}^t$	=	total stress
$\delta_{ij}$	=	Kroneker delta
$u$	=	suction

In equation 3.1, the material property or constant  $k_6$  is the suction term,  $u\delta_{ij}$ .

### 3.1.2 Poisson's Ratio.

Equation 3.1 has been used extensively to represent pavement material behavior by the highway industry, but with a constant Poisson's Ratio. However, Poisson's Ratio increases with increasing stress ratio ( $\sigma_1/\sigma_3$ ) for granular materials and decreasing resilient moduli for bituminous materials reaching values greater than 0.5 (corresponding to dilation). The formulation of the relationship between resilient modulus and Poisson's Ratio follows that given by Lade and Nelson (1987) within the thermodynamic constraint noted above, i.e., the thermodynamic laws are always satisfied and energy is not generated during any loading-unloading cycle.

According to the principle of conservation of energy for elastic material, the work must be independent of the load path. The total work ( $W_T$ ) for a complete loading cycle ABCDA is given by (Figure 3.2):

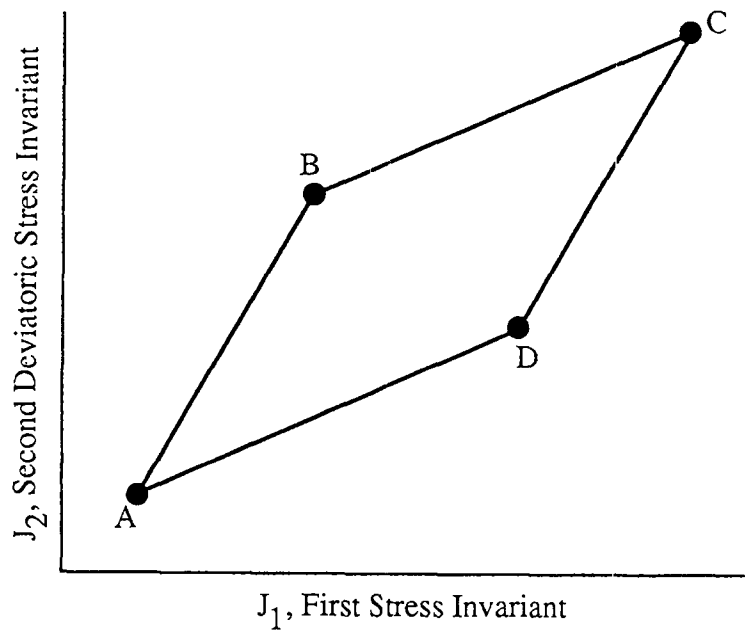


**Figure 3.2 Stress Path for Given Loading Cycle**

$$W_T = W_{ABC} + W_{CDA} = \int \left( \frac{I_1 dI_1}{9K} + \frac{dJ_2}{2G} \right) \quad (3.3)$$

where:  $W_{ABC}$  = Elastic work per unit volume along stress path ABC  
 $I_1$  = First stress invariant =  $\sigma_1 + \sigma_2 + \sigma_3$   
 $J_2$  = Second deviatoric stress invariant =  $(3 \tau_{oct}^2)/2$   
 $K, G$  = Bulk and shear moduli, respectively.

Using the path independence of the elastic work, the following partial differential equation relates the resilient modulus ( $E_R$ ) and Poisson's Ratio ( $\nu$ ) to the stress state, as defined by  $I_1$  and  $J_2$ :

$$2/3 \frac{\partial \nu}{\partial J_2} + \frac{1}{I_1} \frac{\partial \nu}{\partial I_1} = - \frac{1-2\nu}{3} \left( \frac{\partial \ln E_R}{\partial J_2} \right) + \frac{1+\nu}{I_1} \left( \frac{\partial \ln E_R}{\partial I_1} \right) \quad (3.4)$$

A solution to the partial differential equation was obtained for Poisson's Ratio using Equation 3.1, as a solution for the resilient modulus. Substituting Equation 3.1 into the above equation leads to a partial differential equation where  $\nu$  is the dependent variable,  $I_1$  and  $J_2$  are the independent variables, and  $k_2$  and  $k_3$  are material constants. The resulting partial differential equation, which is also called the first order quasi-linear equation, is:

$$2/3 \frac{\partial \nu}{\partial J_2} + \frac{1}{I_1} \frac{\partial \nu}{\partial I_1} = \nu \left[ \frac{2}{6} \left( \frac{k_3}{J_2} \right) + \frac{k_2}{I_1^2} \right] - \frac{1}{6} \frac{k_3}{J_2} + \frac{k_2}{I_1^2} \quad (3.5)$$

The problem is reduced to the solution of the following system of an ordinary differential equation:

$$\frac{dx}{1/x} + \frac{dy}{2/3} = \frac{dz}{z \left[ \frac{k_2}{x^2} + \frac{2k_3}{6y} \right] + \left[ \frac{k_2}{x^2} - \frac{1}{6} \frac{k_3}{y} \right]} \quad (3.6)$$

where:  $x$  =  $I_1$   
 $y$  =  $J_2$

$$z = v$$

Two general solutions, including the boundary conditions, were obtained for this system of differential equations:

$$U_1 = 3y - x^2 \quad (3.7)$$

$$U_2 = \frac{Z}{X^{k_2} Y^{k_3/2}} - \frac{3^{k_3/2}}{2(X^2 - 3Y)^{(k_2+k_3)/2}} \left[ -k_2 B_v \left( \frac{k_2+k_3}{2}, \frac{-k_3}{2} + 1 \right) + k_3 B_v \left( \frac{k_2+k_3}{2}, -\frac{k_3}{2} \right) \right] \quad (3.8)$$

where:

$$V = 1 - \frac{3Y}{X^2} \quad (3.8a)$$

$B_v(a,b)$  is the incomplete Beta function from the experimental test results. The SHRP A-005 contractor found that  $U_1$  and  $U_2$  were related through an exponential form (3.9), as shown below:

$$U_2 = k_4(-U_1)^{k_5} \quad (3.9)$$

where  $k_4$  and  $k_5$  are material properties or constants. When  $k_4$  and  $k_5$  are determined by regression analyses from the results of the accelerated laboratory tests, Poisson's Ratio,  $\nu$ , is expressed by:

$$\nu = \theta^{k_2} \left( \frac{3}{2} \tau oct^2 \right)^{k_3/2} \left[ k_4 U^{k_5} + C u^{(k_2+k_3)/2} B \right] \quad (3.10)$$

where:  $C = \text{Constant}$

$$u = \theta^2 - 9 \left( \tau \frac{oct^2}{2} \right) \quad (3.10a)$$

$$B = -k_2 B_v \left( \frac{k_2+k_3}{2}, \frac{-k_3}{2} + 1 \right) + \frac{k_3}{2} B_v \left( \frac{k_2+k_3}{2}, -\frac{k_3}{2} \right) \quad (3.10b)$$

The material constants or coefficients,  $k_1$  through  $k_6$ , are determined from the loaded and recovery part of the laboratory test at a specific temperature and test condition (stress - state). To determine the effect of temperatures and stress-state on the modulus, the tests are performed over a series of temperatures and stress conditions.

## 3.2 Time-Dependency Properties: The Viscoelastic Model

Unlike granular and fine-grained soils, asphalt concrete mixtures do exhibit a visco-elasto-plastic behavior. These materials typically behave as nonlinear elastic or viscoelastic materials at low temperatures, and are nonlinear visco-elasto-plastic at high temperatures. For the case of linear viscoelasticity, an appropriate physical model can be selected that best fits the test results or the power law can be simply used in its general form. For the non-load related distress (thermal cracking), a Maxwell model was selected because the assumption of a linear viscoelastic material is reasonable at cold temperatures. For the load related distresses (rutting and fatigue cracking), however, use of the power law was selected by the SHRP A-005 contractor. The power law is:

$$\epsilon(t) = \left[ \frac{d_o + d_1 a t^m}{1 + a t^m} \right] \sigma_o \quad (3.11)$$

This was simplified by the A-005 contractor to the following form:

$$\epsilon(t) = (d_o + d_1 t^m) \sigma_o \quad (3.12)$$

where:  $\epsilon(t)$  = strain function describing the response of the material to a step function loading sequence  
 $t$  = time  
 $\sigma_o$  = amplitude of the applied stress  
 $d_o, d_1, a, m$  = material properties

### 3.2.1 Load Related Response Model.

For the general form of the power law, the strain is limited to  $d_1 \sigma_o$ ; however, in the simplified form, the strain increases with time,  $t$ , without any upper limit. This simplified form (Equation 3.12) is preferred because of the ease of implementation and mathematical treatment. As an example, when the load function is sinusoidal, it is easy to use the Laplace Transform to obtain the real and imaginary parts of the creep compliance function  $D(t)$ :

$$D(t) = d_o + d_1 t^m \quad (3.13)$$

$$D^*(\omega) = d_o + d_1 \Gamma(1 + m) \omega^{-m} \cos\left(\frac{\pi m}{2}\right) \quad (3.14)$$

$$D^{**}(\omega) = d_1 \Gamma(1 + m) \omega^{-m} \sin\left(\frac{\pi m}{2}\right) \quad (3.15)$$

where:  $\omega$  = frequency  
 $\Gamma$  = Gamma function

In the Superpave system, the three parameters  $d_o$ ,  $d_1$  and  $m$  are determined from an analysis of the frequency sweep test results. In the case of nonlinear visco-elasto-plasticity, repeated creep tests are used to separate the strain into the four basic components that were previously discussed. The instantaneous response is time independent and includes both an elastic (recoverable) and plastic (irrecoverable) component. The time dependent response under a sustained or constant load also includes two components; i.e., a viscoelastic and viscoplastic component. Upon removal of the load, the instantaneous response only includes the elastic response and the time dependent response after unloading is due to viscoelasticity only. With time, the response of the material approaches the plastic and viscoplastic components, of which both are irrecoverable. Using the power law for describing the viscoelastic and viscoplastic components, the creep compliance can be described as:

$$D(t) = D_e + D_p + D_{ve} t^m + D_{vp} t^n \quad (3.16)$$

where:  $D_e$  = elastic component  
 $D_p$  = plastic component  
 $D_{ve}, m$  = viscoelastic component parameters  
 $D_{vp}, n$  = viscoplastic component parameters

The above expression states that the total strain,  $D(t) \sigma_o$ , continues to increase with time at a uniform or constant rate. However, most materials can exhibit instability beyond some critical strain value at which the deformation increases at an accelerating rate. This type of response is typically referred to as tertiary creep, which occurs at some level of accumulated viscoplastic deformation. Thus, the SHRP A-005 contractor added the following term to the creep-compliance function:

$$\Delta\epsilon(t) = b \left[ \frac{\epsilon_{vp}(t)}{\epsilon_{vp}^c} - 1 \right] \left[ \frac{\epsilon_{vp} t}{\epsilon_{vp}^c} \right]^p \quad (3.17a)$$

where:

$$\epsilon_{vp} = D_{vp} t^n \sigma_o \quad (3.17a)$$

- $\Delta\epsilon(t)$  = The additional total strain component related to the tertiary strain  
 $\epsilon_{vp}$  = Viscoplastic strain component  
 $\epsilon_{vp}^c$  = Critical viscoplastic strain which is mixture dependent  
 $b, p$  = Material parameters that are mixture dependent

Under repeated loads, the so-called damage or irrecoverable strain component can be expressed in an exponential form as follows:

$$\epsilon_p(N) = D_p \sigma_o N^\mu \quad (3.18)$$

and

$$\epsilon_{vp}(N) = D_{vp}(t)^n \sigma_o N^\nu \quad (3.19)$$

- where:  $\epsilon_p(N)$  = Plastic strain component accumulated after N load applications  
 $\epsilon_{vp}(N)$  = Viscoplastic strain component accumulated after N load applications  
 $\mu, \nu$  = Material parameters that are mixture dependent and determined by regression analyses of laboratory test data.

It is seen that a complete characterization of the nonlinear viscoelastic plasticity requires eight parameters in addition to the elastic ( $D_e$ ) and plastic ( $D_p, \mu$ ) components. Six of these parameters are constants ( $m, n, \nu, b, p, \epsilon_{vp}^c$ ) and the other two ( $D_{ve}, D_{vp}$ ) are stress dependent. In order to retain the performance model restrictions discussed at the beginning of this chapter, it is not possible to use the above relations directly in the pavement response model. A quasi-nonlinear elastic model without the time variable, however, can be used for evaluating a mixture's response to an applied load. Thus, an elasto-plastic formulation was used.

The material response model is based on the quasi-nonlinear elasticity using the resilient model previously discussed (Equation 3.1). The plasticity part is considered using Vermeer's model, which will be discussed in the section on plasticity. In summary, the visco-elastic and visco-plastic parts of the response components are considered, but at a specific time interval because the computations are time intensive.



### 3.2.2 Non-Load Related Response Model

The viscoelastic properties of an asphalt concrete material control the state of stress within the material during cooling at relatively low temperatures (0°C and below). The time and temperature-dependent relaxation modulus of a mixture is a viscoelastic property of the material that is needed to compute thermal stresses according to the following constitutive equation:

$$\sigma(\xi) = \int_0^{\xi} E(\xi - \xi') \frac{d\varepsilon}{d\xi'} d\xi' \quad (3.20)$$

where:

$\sigma(\xi)$	=	stress at reduced time $\xi$
$E(\xi - \xi')$	=	relaxation modulus at reduced time $\xi - \xi'$
$\varepsilon$	=	strain at reduced time $\xi$ ( $= \alpha (T(\xi') - T_0)$ )
$\alpha$	=	linear coefficient of thermal contraction
$T(\xi')$	=	pavement temperature at reduced time $\xi'$
$T_0$	=	pavement temperature when $\sigma = 0$
$\xi'$	=	variable of integration

A generalized Maxwell model was selected to represent the viscoelastic properties of the asphaltic concrete mixture. Mathematically, the generalized Maxwell model is expressed according to the following Prony series expansion:

$$E(\xi) = \sum_{i=1}^{N+1} E_{ie}^{-\xi/\lambda_i} \quad (3.21)$$

where:

$E(\xi)$	=	relaxation modulus at reduced time $\xi$
$E_i, \lambda_i$	=	Prony series parameters for master relaxation modulus curve

This function describes the relaxation modulus as a function of time at a single temperature, which is generally known as the reference temperature. The function defined at the reference temperature is called the master relaxation modulus curve. Relaxation moduli at other temperatures are determined by using the method of reduced variables (time-temperature superposition), which simply means that the mixture is assumed to behave as a thermorheologically simple material. Relaxation moduli at other temperatures are determined by replacing real time (i.e., time corresponding to the temperature of interest) with reduced time (i.e., time corresponding to the temperature at which the relaxation modulus is defined) according to the following equation:

$$\begin{aligned}
\xi &= \text{reduced time} = t/a_T & (3.22) \\
t &= \text{real time} \\
a_T &= \text{temperature shift factor}
\end{aligned}$$

The relaxation modulus function is obtained by transforming the following time-dependent creep compliance function, which is determined by performing creep tests at multiple temperatures:

$$D(\xi) = D(0) + \sum_{i=1}^N D_i (1 - e^{-\xi/\tau_i}) + \frac{\xi}{\eta_v} \quad (3.23)$$

where:

$D(\xi)$	=	creep compliance at reduced time $\xi$
$\xi$	=	reduced time = $t/a_T$
$a_T$	=	temperature shift factor
$D(0), D_i, \tau_i, \eta_v$	=	Prony series parameters

### 3.3 Inelastic Properties: The Plasticity Model

The plasticity theory is developed to characterize the nonlinear and inelastic behavior of materials. In the concept of plasticity, the development of the incremental stress-strain relation is based on three fundamental assumptions. These assumptions are:

1. The existence of initial and subsequent yield surfaces,
2. The formulation of an appropriate loading rule that describes the evolution of subsequent loading surfaces, and
3. A flow rule which specifies the general form of the stress-strain relationship.

As stated in the previous section, the behavior of asphalt concrete follows that of a nonlinear visco-elasto-plastic model. The time dependence is important and should not be neglected. However, to ensure that the pavement response model is practical for day-to-day mixture design use, the time dependence of the material response is taken into account by using material properties corresponding to a given loading and unloading time. This obviously is an oversimplification of the pavement structure, but is practical and believed to provide a reasonably accurate estimate of the pavement response.

The behavior of various pavement materials is basically inelastic, because upon load removal, unloading follows an entirely different path from that followed by the loading phase. It is not easy to define the unloading behavior with nonlinear inelasticity models. This difficulty can be overcome, however, by the introduction of the incremental theory of an

initial yield surface, the evolution of subsequent loading surfaces (the hardening rule), and the formulation of an appropriate flow rule.

### 3.3.1 Elastoplasticity Formulation.

The deformation under loading for the load related response model is assumed to be composed of two parts, the elastic and plastic components, or the recoverable and the unrecoverable parts, respectively. Thus, the total strains can be expressed by Equation 3.24, which is a reduced form of Equation 3.16 (i.e., defined at a specific loading/unloading time).

$$\epsilon = \epsilon^e + \epsilon^p \quad (3.24)$$

where:  $\epsilon$  = total strain tensor  
 $\epsilon^e$  = elastic (recoverable) strain tensor  
 $\epsilon^p$  = plastic (unrecoverable) strain tensor

In some cases, the unrecoverable component is nonexistent (or not noticeable) until the stress condition reaches a given limit. In incremental terms, this can be stated as follows: *plastic deformation takes place when the stress increment is beyond the above limit.*

This can be expressed through the yield function. Plastic deformation occurs when:

$$F(\sigma, R) = 0$$

$$dF(\sigma, R) = 0$$

and

$$\left(\frac{\partial F}{\partial \sigma}\right)^T d\sigma \geq 0$$

where:  $F(\sigma, R)$  = yield function  
 $\sigma$  = stress tensor  
 $R$  = hardening parameter

It should be mentioned that when  $F(\sigma, R) < 0$  or  $F(\sigma, R) = 0$  and  $\frac{\partial F}{\partial \sigma} d\sigma < 0$ , the

material is assumed to behave elastically. The hardening parameter determines the elastic domain extent, or in other terms, the expansion of the yield surface. In incremental terms,

deformation or strain can be expressed as:

$$d\epsilon = d\epsilon^e + d\epsilon^p \quad (3.25)$$

where:  $d\epsilon$  = total strain increment  
 $d\epsilon^e$  = elastic strain increment  
 $d\epsilon^p$  = plastic strain increment

The elastic strain increment is obtained from the following relationship:

$$d\epsilon^e = d\epsilon - d\epsilon^p = D^{-1}d\sigma \quad (3.26)$$

where:  $D$  = matrix of elastic parameters which are constant in linear elasticity and dependent upon the stress or strain state in nonlinear elasticity.

The plasticity strain increment is obtained from the plastic potential as follows:

$$d\epsilon^p = \lambda \frac{\partial G(\sigma, R)}{\partial \sigma} \quad (3.27)$$

where:  $\lambda$  = a coefficient of proportionality  
 $G(\sigma, R)$  = plastic potential (=  $F(\sigma, R)$  in the case of associative plasticity)

Equation (3.27) defines the flow rule and states that the plastic strain increment is proportional to the stress gradient of the surface termed the plastic potential. The  $\lambda$ -coefficient may be obtained as follows.

$$\lambda = \frac{\left(\frac{\partial F}{\partial \sigma}\right)^T D}{H + \left(\frac{\partial F}{\partial \sigma}\right)^T D \left(\frac{\partial G}{\partial \sigma}\right)} d\epsilon \quad (3.28)$$

The total strain increment can be obtained by substituting Equations (3.27) and (3.28) into Equation (3.26) and solving the resulting equation. The plastic strain increment is then obtained from Equation (3.25).

An important component of the elasto-plastic approach is the failure law. This law constitutes an upper limit of the yield function and determines the shapes of the yield function and the plastic potential. In this study, the Vermeer model has been adopted. The Vermeer model is characterized by a few parameters which may be easily linked to traditional soil constants and satisfies the requirements for the practical applications. In the Vermeer model,

the total strain increments are divided into two inelastic components: a plastic cone component, and plastic cap component. Each strain component is calculated separately. The elastic strain is calculated by the resilient model, the plastic cap strain by a plastic stress-strain theory involving a cap-type yield surface, and the plastic cone strain by a stress-strain theory which involves a conical yield surface. The Vermeer model is discussed in greater detail in the following section.

### 3.3.2 *The Vermeer Model.*

The Vermeer Model is based on the following assumptions (Vermeer, 1982, and Tadjbakhsh and Frank, 1985):

- (a) *The material is isotropic.*
- (b) *The model is based on isotropic hardening.*
- (c) *The strain is composed of three parts, i.e.*

$$\epsilon = \epsilon^e + \epsilon^{ps} + \epsilon^{pc}$$

where:

- $\epsilon$  = total strain
- $\epsilon^e$  = elastic strain
- $\epsilon^{ps}$  = plastic strain due to shear
- $\epsilon^{pc}$  = plastic strain due to isotropic consolidation

The elastic behavior is nonlinear with a Poisson's ratio of zero. It is worth mentioning that all three parts of the total strain include a volumetric component which can be dilation for  $\epsilon^{pc}$  and  $\epsilon^{ps}$ .

(d) The Matsuoka and Nakai failure law is used, namely:

$$f_p = -3p I_2 + A_p I_3 + 0 \quad (3.29)$$

where:

$$p = -\frac{1}{3} (\sigma_1 + \sigma_2 + \sigma_3) = \frac{1}{3} (\sigma_r + \sigma_z + \sigma_\theta) \quad (3.29a)$$

$$I_2 = -(\sigma_1 \sigma_2 + \sigma_2 \sigma_3 + \sigma_3 \sigma_1) = -(\sigma_r \sigma_z + \sigma_z \sigma_\theta + \sigma_\theta \sigma_r - \tau_{rz}^2) \quad (3.29b)$$

$$I_3 = \sigma_1 \sigma_2 \sigma_3 = \sigma_r \sigma_\theta \sigma_z - \tau_{rz}^2 \sigma_\theta \quad (3.29c)$$

$$A_p = \frac{(9 - \sin^2 \Phi_p)}{\cos^2 \Phi_p} \quad (3.29d)$$

$\phi_p$  = peak friction angle (at failure)

The Matsuoka-Nakai criterion law can be viewed as a smooth extension of the Mohr-Coulomb law without the apexes in its plot in the deviatoric plane of the principal stress space (Matsuoka and Nakai, 1985, and Houlsby, 1986).

(e) The yield function for  $e^{ps}$  is given by:

$$F_{ps} = -3pI_2 + A(x)I_3 = 0 \quad (3.30)$$

where:

$$A(x) = \frac{27}{2h(x) + 3} \cdot \frac{3 + h(x)}{3 - h(x)} = \frac{9 - \sin^2 \Phi_m}{\cos^2 \Phi_m} \quad (3.30a)$$

$$h(x) = \sqrt{\left(\frac{1}{2}x\right)^2 + cx} - \frac{1}{2}x \quad (3.30b)$$

$$x = \gamma^p \frac{2G_0}{P_0} \left(\frac{P_0}{p}\right)^\beta \quad (3.30c)$$

$$\begin{aligned}
\gamma^p &= \text{plastic shear strain} \\
x &= \text{normalized plastic distortion} \\
P_0 &= \text{pressure of reference for expressing laws in nondimensional form} \\
G_0 &= \text{shear modulus in simple shear test at isotropic stress of } p_0 \\
\phi_m &= \text{mobilized angle of friction } (\leq \phi_p) \\
c &= 6 \sin \phi_p / (3 - \sin \phi_p) \\
\beta &= \text{material parameter}
\end{aligned} \tag{3.30d}$$

It should be noted that at failure  $\phi_m \rightarrow \phi_p$ ,  $\gamma^p \rightarrow \infty$ ,  $x \rightarrow \infty$ , and  $h(\infty) = c$ . The plastic shear strain  $\gamma^p$  is the hardening parameter.

(f) *The simplified shear plastic potential which includes the dilatancy angle can be defined as:*

$$G_{ps} = \sqrt{\frac{2}{3}} q + \frac{4 \sin \psi_m}{\sqrt{6 + 2 \sin^2 \psi_m}} \tag{3.31}$$

where:

$$q = \frac{1}{\sqrt{2}} [(\sigma_r - \sigma_\theta)^2 + (\sigma_\theta - \sigma_z)^2 + (\sigma_z + \sigma_r)^2 + 6\tau_{rz}^2]^{\frac{1}{2}} \tag{3.31a}$$

$$\sin \psi_m = \frac{\sin \Phi_m - \sin \Phi_{cv}}{1 - \sin \phi_{cv} \sin \phi_m} \tag{3.31b}$$

$\phi_{cv}$  = the friction angle at constant volume

(g) *The volumetric flow is associative. The yield function for  $\epsilon^{pc}$  (also the volumetric plastic potential) is given by:*

$$F_{pc} = G_{pc} = \epsilon_0^c \left( \frac{p}{p_0} \right)^\beta - e^{pc} \tag{3.32}$$

where:

$\epsilon_0^c$  = material constant

$\epsilon^{pc}$  = second hardening parameter, representing the plastic volumetric strain given by

$$\epsilon^{pc} = \sum_{i=1}^{incr} d\epsilon_i^{pc} \tag{3.32a}$$

incr = number of load increments

The model requires five parameters: (1) the peak angle of friction  $\phi_p$ , (2) the friction angle at constant volume  $\phi_{cv}$ , (3) the exponent  $\beta$ , (4) the shear modulus  $G_0$  at  $p_0$ , and (5) the volumetric constant  $\varepsilon_0$ . It should be noted that this model was developed for granular materials with no cohesion. Furthermore, the model relies strongly on the material elastic characteristic, where the shear modulus,  $G_s$ , is expressed as function of the bulk stress (or  $p$ ) as shown in Equation 3.33.

$$G_s = G_0 \left(\frac{p}{p_0}\right)^{1-\beta} \quad (3.33)$$

The Poisson's ratio effect on the shear modulus is nil. According to Vermeer (1985),  $2G_0$  is the initial slope of the  $\gamma - q$  curve in a test with  $p = p_0$ .

A modification of the theory such as the one proposed by Vermeer and de Brost (1984) was selected by the SHRP A-005 contractor. The modification is based on a translation of the principal stress space along the hydrostatic axis by adding a constant stress to the normal stresses, i.e.:

$$\bar{\sigma}_{ij} = \sigma_{ij} - c \cot \phi_p \delta_{ij} \quad (3.34)$$

where:  $\bar{\sigma}$  = transformed stress tensor  
 $\sigma_{ij}$  = actual stress tensor  
 $c$  = cohesion, either true or apparent

The above translation is needed only for the stress values used in conjunction with the yield function and plastic potential, not with the modulus computation in equation 3.33.

When  $k_3 = 0$ , in the general elastic modulus, equation 3.1 reduces to equation 3.34 with  $k_2 = 1 - \beta$ ; when  $k_2 = 0$  corresponding to cohesive materials, the two equations are totally different. The use of equation 3.1 in Vermeer's model together with the extension to cohesive materials requires a modification of the formulation. In developing the model, Vermeer used equation 3.34 for the elastic response and an hyperbolic relation between the total shear strain and stress ratio. In mathematical form:



$$\gamma^e = \frac{q/2}{G} \quad (3.35)$$

$$\gamma = B \frac{c\eta}{c - \eta} \quad (3.36)$$

where:  $\eta = q/p$  = deviatoric to isotropic stress ratio  
 $\gamma^e, \gamma$  = elastic and total shear strain  
 $B$  = material parameter, describing the reciprocal of the initial modulus in  $\eta - \gamma$  curve

The function used for  $B$  was taken from Hansen (1965) as a power law of the form:

$$B = \frac{p_0}{2G_0} \left( \frac{p}{p_0} \right)^\beta \quad (3.37)$$

Using equations 3.34, 3.35 and 3.36, Vermeer arrived at an expression for  $\gamma^p$  as follows:

$$\gamma^p = \gamma - \gamma^e = \frac{p_0}{2G_0} \left( \frac{p}{p_0} \right)^\beta \frac{\eta^2}{c - \eta} \quad (3.38)$$

The above equation forms the basis for the yield function shown in equations 3.32 and 3.32a. Substituting equation 3.1 into equation 3.35 leads to a function for  $\gamma^p$  which includes  $k_2$  and  $k_3$  in both the free term and the exponent of  $\eta$  in equation 3.38. A simple yield function like equations 3.32 and 3.32a could not be derived, limiting the use of the model to granular materials with  $k_3$  equal to zero. However, the model could be used for all pavement materials if the following assumptions are made.

- (a) The shape of the  $\gamma^p$  - function remains given by Equation (3.30d); thus neglecting the effect of the shear term in equation 3.1;
- (b) The parameter  $p$  in equations 3.30 and 3.38 is assumed to be an independent variable that can be determined from the test results. However, it should be set to the value used in equation 3.34 when a material with  $k_3 = 0$  is encountered.

The extended model requires five parameters in addition to the elastic parameters, namely the peak friction angle, the angle of friction at zero volume change, the cohesion, the  $\varepsilon_0^\circ$  - parameter and the  $\beta$  - parameter to be used in equation 3.32 and 3.38.

### 3.4 Fracture Properties: The Strength Model

The previous constitutive equations are used to predict the response of a material from an applied load, but for the case with little or no damage (no localized fracture within the material). For example, it is well known that a hysteresis loop is observed in a stress-strain diagram when a viscoelastic material is subjected to cyclic loading. However, according to Schapery's theory, this hysteresis loop will not be present if the physical stresses are plotted with the corresponding pseudo-strains provided that the damage growth in the material is negligible. But, when the damage growth is not negligible, a damage parameter has to be included to satisfy the above statements.

To describe the mixture's response to continued loading where damage or fracture becomes important, an evaluation of the tensile strength test data was performed using Schapery's theory for damage growth and fracture in composite materials. The constitutive equation expressing stress in terms of pseudo-strain and a damage parameter is:

$$\sigma = I \epsilon_o S_p \left[ 1 + g_1 \epsilon_o + g_2 \epsilon_o^2 \right] \left[ 1 + f_1 S_p + f_2 S_p^2 \right] \quad (3.39)$$

where:  $\sigma$  = stress

$I, g_1, g_2, f_1, f_2$  = model parameters determined from the data

$I$  = Initial stiffness or tangent modulus.

$$\epsilon_o = \frac{1}{E_R} \int_0^t E(t-\tau) \frac{d\epsilon}{d\tau} d\tau \quad (3.39a)$$

$$S_p = \left[ \int_0^t |\epsilon_o|^p dt \right]^{1/p} \quad (3.39b)$$

$p$  = A model parameter

$S_p$  = Damage parameter from Schapery's Theory and is less than 1.0.

$E_R$  = A constant with units of modulus

$E(t)$  = The relaxation modulus function

$$E(t) = E_0 + E_1 t^m \quad (3.39c)$$

The model coefficients of  $E_0$ ,  $E^1$  and  $m$  are found using data from the tensile frequency sweep tests. This constitutive equation was used to determine the damage parameter from tensile strength data that provided an optimum fit of the data for the tensile frequency sweep tests at different temperatures.

## 4

# The Pavement Response Model

## 4.1 Finite Element Program

In most geomechanics and pavement problems, the closed form solutions to the governing differential equation are difficult to obtain. Therefore, various numerical techniques have been adopted to derive the solutions to these types of problems. Of course, the finite element method has proven to be a highly efficient and versatile numerical technique. The multifaceted advantages of the finite element method lie in its capability of introducing nonlinearity in the solution of the boundary value problem and of handling inhomogeneity in irregular geometry effectively. Furthermore, this method allows one to include such factors as in-situ stress, different types of loading, stress paths and interface conditions.

A 2-dimensional finite element code for material nonlinearity has been adopted by Owen and Hinton (1980) for the plain stress, plain strain and axisymmetric problems. The procedures and codes used in the finite element model are derived from their work with a number of modifications which include: the mesh generation, in-situ stress, implementation of the different constitutive models, nonsymmetry solver and the flexible boundary condition. In the pavement performance model, only the axisymmetrical condition is used. The formulation of the finite element method can be obtained by the use of the principle of virtual work. The primary response model is based on a 2-D axisymmetric F.E. (finite element) program. A four node element is used with one Gauss point for integration, and incremental loading with iterations for convergence.

## 4.2 The Incremental Stress-Strain Relation

The constitutive equation in the resilient modulus model is a sequent modulus. In order to incorporate this model with the incremental finite element program, the incremental stress-strain relation for this model is presented. The strain-stress relation for the generalized Hooke's Law can be expressed by the mathematical description of the variable moduli in terms of the incremental stress-strain relations, or in mathematical form:

and

$$\begin{aligned} d_p &= k d\epsilon_{kk} \\ ds_{ij} &= 2G de_{ij} \end{aligned}$$

Where:  $d_p$  is the mean hydrostatic stress,  
 $d\epsilon_{kk}$  is the volumetric strain increments, and  
 $ds_{ij}$  and  $de_{ij}$  are the deviatoric stress and strain increments, respectively.

Therefore, equations 3.1, 3.8 and 3.9 were used to derive the compliance matrix relating the stress and strain increments. In other words:

$$d\epsilon = [D] d\sigma \quad (4.1)$$

where:  $d\epsilon$  = vector of strain increments  
 $d\sigma$  = vector of stress increments  
 $[D]$  = compliance matrix of coefficients

The compliance matrix of coefficients is obtained by taking the derivatives of the stress-strain relations. Using the chain rule of differentiation, the  $\epsilon_x$  increment (in the x, y, z coordinate system) is given by:

$$d\epsilon_x = \sum \frac{d\epsilon_x}{d\sigma_i} d\sigma_i \quad (4.2)$$

or

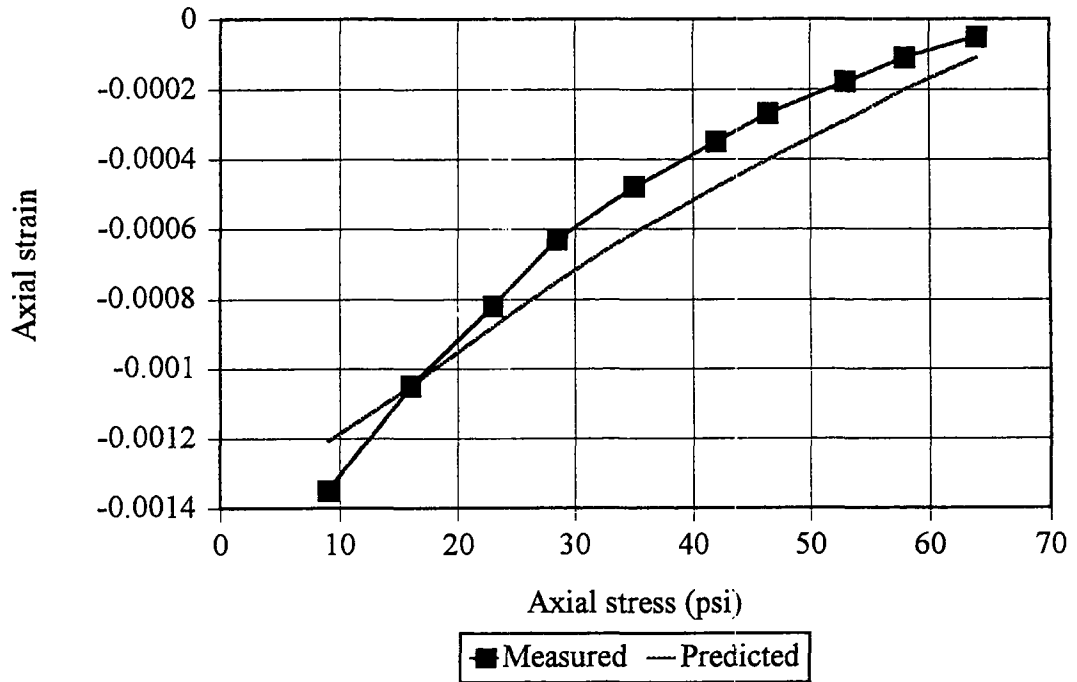
$$\begin{aligned} d\epsilon_x = & \frac{\partial \epsilon_x}{\partial \sigma_x} d\sigma_x + \frac{\partial \epsilon_x}{\partial \sigma_y} d\sigma_y + \frac{\partial \epsilon_x}{\partial \sigma_z} d\sigma_z + \frac{\partial \epsilon_x}{\partial \tau_{xy}} d\tau_{xy} \\ & + \frac{\partial \epsilon_x}{\partial \tau_{yx}} d\tau_{yx} + \frac{\partial \epsilon_x}{\partial \tau_{zx}} d\tau_{zx} \end{aligned} \quad (4.3)$$

The above formulation was included into the finite element program for axisymmetric conditions.

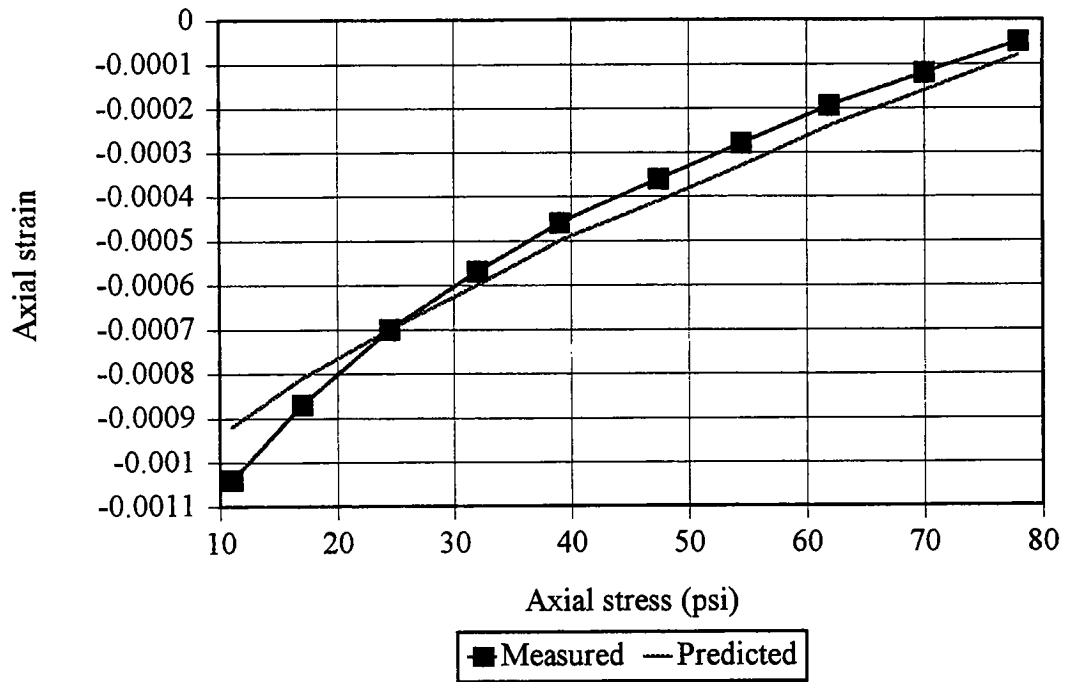
Since the resilient modulus is the unloading modulus of the material, the fitting should be used based on the unloading curve of the test. This model is used to predict the behavior of various materials and the prediction of the test results have been found to agree very well. The material properties of the asphalt concrete for the  $k$ -coefficients in the resilient model (equation 3.1) are obtained by fitting the unloading portion of the uniaxial compression test, the volumetric compression test and the simple shear test.

Figure 4.1 shows the comparison of the observed and predicted stress-strain response of the uniaxial test in the unloading portion. It can be seen that the predictions and test results agree very well. The comparison of the observed and predicted stress-strain response of the volumetric test is shown in Figure 4.2, with similar correspondence between the observations and predictions. Figure 4.3 is a plot of the stress-strain curve for the (Superpave) simple shear at constant height test obtained from the experiment and predicted by the model.

These comparisons show that the resilient model can predict the response of asphalt concrete mixes very well, with the exception of the shear test. One of the possible reasons for this greater error or divergence between observations and predictions from the simple shear test is that there is an anisotropic behavior that occurs during the shear loading. The resilient model may be unable to model the anisotropic behavior during this type of loading condition.



**Figure 4.1 Comparison of predictions and observations for uniaxial strain test using the  $k_1$ - $k_5$  model on asphalt concrete**



**Figure 4.2 Comparison of predictions and observations for volumetric compression test using the  $k_1$ - $k_5$  model on asphalt concrete**



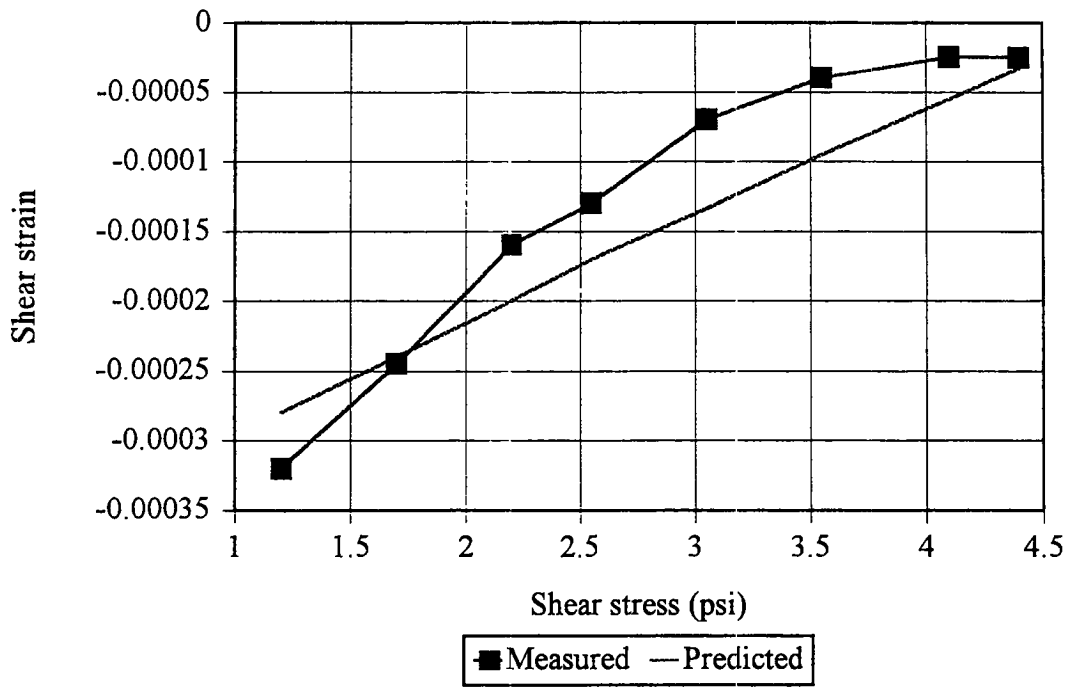


**Figure 4.3 Comparison of predictions and observations for shear test using the  $k_1$ - $k_5$  model on asphalt concrete**

## 5

# Thermal Cracking Model Formulation

## 5.1 Calculation of Thermal Stresses

The pavement response model predicts the thermal stresses within the pavement system using the material properties, pavement structural information, and pavement temperature predictions from the environmental effects model. This will be discussed in greater detail in chapter 9. The thermal response model is based upon a one-dimensional constitutive equation with an approximate means to model the two-dimensional stress distribution within the asphalt layer. Thermal stress predictions within the asphalt layer are based upon Boltzmann's Superposition Principle for linear viscoelastic materials:

$$\sigma(\xi) = \int_0^{\xi} E(\xi - \xi') \frac{d\epsilon}{d\xi'} d\xi' \quad (5.1)$$

where:	$\sigma(\xi)$	=	stress at reduced time $\xi$
	$E(\xi - \xi')$	=	relaxation modulus at reduced time $\xi - \xi'$
	$\epsilon$	=	strain at reduced time $\xi$ ( $= \alpha (T(\xi') - T_0)$ )
	$\alpha$	=	linear coefficient of thermal contraction
	$T(\xi')$	=	pavement temperature at reduced time $\xi'$
	$T_0$	=	pavement temperature when $\sigma = 0$
	$\xi'$	=	variable of integration

The equation essentially models the asphalt layer as a uniaxial rod. The constitutive equation is written in terms of reduced time,  $\xi$ , because time-temperature superposition is being used to represent the creep compliance and relaxation modulus curves. The use of time-temperature superposition means that the asphalt mixture is modeled as a thermorheologically simple material. With a change of variables, the equation is written in terms of real time,  $t$ , as follows:

$$\sigma(t) = \int_0^t E[\xi(t) - \xi'(t')] \frac{de}{dt'} dt' \quad (5.2)$$

Using the Prony series representation of  $E(\xi)$ , the following finite difference solution to the above equation has been developed:

$$\sigma(t) = \sum_{i=1}^{N+1} \sigma_i(t) \quad (5.3)$$

and:

$$\sigma_i(t) = e^{-\Delta\xi/\lambda_i} \sigma_i(t-\Delta t) + \Delta\epsilon E_i \frac{\lambda_i}{\Delta\xi} (1 - e^{-\Delta\xi/\lambda_i}) \quad (5.4)$$

$\Delta\epsilon$  and  $\Delta\xi$  are the changes in strain and reduced time, respectively, over time  $t-\Delta t$  to  $t$ , and all other variables are as previously defined. It should be noted that the use of a one-dimensional constitutive model was necessitated by the fact that stress predictions must be made at small time intervals over analysis periods of many years using a personal computer. Obviously, the stresses vary with depth due to a temperature gradient within the layer; finite element modeling has confirmed this phenomenon. Previous thermal cracking models have based their stress predictions solely on the pavement temperature at the surface, and have assumed that these stresses exist throughout the layer. In fact, the stresses reduce with increased depth, and thus such assumptions overpredict the amount of damage within the pavement for a given temperature cycle.

In lieu of using a more accurate two or three-dimensional model, an approximate means has been developed to estimate this stress distribution using the one-dimensional model. Temperatures are predicted at multiple depths (nodes) within the layer using the environmental effects model. Typically the nodes are located at 2-inch intervals. For each of these temperature nodes, stresses are predicted using the one-dimensional model, thus establishing an approximate stress distribution with depth. This stress distribution is used as input to the crack depth or fracture model. The fracture model uses the stress at the current location of the crack tip to calculate the crack advancement during the next temperature cycle.

## 5.2 Pavement Distress Model

The pavement distress model consists of three primary parts: the stress intensity factor model, the crack depth (fracture) model, and the crack amount model. The stress intensity factor model predicts the stress at the tip of a local vertical crack using the far-field stress computed by the pavement response model and the pavement structure and material properties. Based upon the stress at the tip of the crack, the crack depth (fracture) model predicts the amount of crack propagation due to the imposed stress. Finally, the crack amount model predicts the number (or frequency) of thermal cracks per unit length of pavement from the depth of the local vertical crack and the assumed crack depth distribution.

### 5.2.1 Stress Intensity Factor Model.

The stress intensity factor model (CRACKTIP) is a two-dimensional finite element (FEM) program that models a single vertical crack in the asphaltic concrete layer via a crack tip element. The CRACKTIP program was developed at the Texas Transportation Institute. The following points are relevant:

- Suitable finite element meshes were identified and side-by-side comparisons of the CRACKTIP finite element program with the ANSYS program and with standard handbook solutions have been performed in order to verify the accuracy of the CRACKTIP program for use in the low temperature cracking model.
- A regression equation has been developed to predict stress intensity factor much faster than is possible using the CRACKTIP finite element program directly. This equation was developed from a set of data generated by the CRACKTIP program using a matrix of input properties that span the ranges of expected values. The regression equation is used in the low temperature cracking model in lieu of the CRACKTIP program.

### 5.2.2 Crack Depth (Fracture) Model.

The Paris law for crack propagation is used to predict the change in depth of a local crack subjected to a given cooling cycle:

$$\Delta C = A(\Delta K)^n \quad (5.5)$$

where:  $\Delta C$  = change in the crack depth due to a cooling cycle  
 $\Delta K$  = change in the stress intensity factor due to a cooling cycle  
 $A, n$  = fracture parameters

The change in crack depth ( $\Delta C$ ) is computed and accumulated on a daily basis to determine the total crack depth as a function of time. As explained in the next section, the crack depth is related to the total amount of cracking by way of a crack depth distribution function. The idea is that material variability along the length of the pavement section will result in different crack depths, even for the same exposure conditions. The crack depth distribution governs how much cracking is observed in a particular section having a specific crack depth computed on the basis of average material properties.

Since it is not practical to perform fracture tests as part of the Superpave mix design procedure, fracture parameters  $A$  and  $n$  must be determined on the basis of material properties measured as part of the specification tests, along with theoretical or experimental relationships between measured properties and fracture parameters  $A$  and  $n$ . Schapery's theory of crack propagation in nonlinear viscoelastic materials ( Schapery, 1984, 1986) indicates that the fracture parameters  $A$  and  $n$  are theoretically related to:

- The slope of the linear portion of the log compliance-log time relationship determined from creep tests;
- The maximum strength or failure limit of the material (determined from the failure test immediately following the creep test); and
- The fracture energy density of the material determined experimentally by monitoring the energy release through crack propagation

Determination of the fracture energy density requires additional, complex testing, which could not be incorporated into a mixture specification scenario. However, experimental results indicate that fairly reasonable estimates of  $A$  and  $n$  can be obtained from the  $m$ -value and the failure limit of the material. Experiments by Molenaar (1983) led to the following relationship:

$$\log A = 4.389 - 2.52 * \log(E * \sigma_m * n) \quad (5.6)$$

where:  $E$  = mixture stiffness, psi  
 $\sigma_m$  = mixture strength, psi

Experiments conducted by Lytton et al. (1990) led to the following relationship:

$$n = 0.8 * \left(1 + \frac{1}{m}\right) \quad (5.7)$$

Both researchers found  $A$  was related to  $n$ , and Lytton found that  $n$  was related to  $m$ . Both of these findings agree with Schapery's theoretical development from nonlinear viscoelastic materials, where Schapery proved that both  $A$  and  $n$  are related to  $m$ . Both the  $m$ -value and

strength for use in these relationships are determined from the laboratory tensile creep and failure test.

### 5.2.3 *Crack Amount Model.*

In order to predict the amount of cracking per unit length of pavement section from the average crack depth and the distribution of crack depths within the section, the following assumptions were made:

- Within a given pavement section there is a maximum number of thermal cracks that can occur and these cracks are uniformly spaced throughout the section (or conversely, there exists a minimum crack spacing beyond which no further cracks will develop). This assumption is supported by actual observations of thermal cracking in the field. Initially, each of these potential cracks starts out as a very small local vertical crack (or flaw, fissure, etc.) at the surface of the asphaltic concrete layer.
- A crack is not counted (or observed) as a crack until the local vertical crack propagates through the entire depth of the asphaltic concrete surface layer. In other words, no contribution is made to the amount of global thermal cracking until the local vertical crack breaks through the surface layer.
- For a given section at a given point in time, each of the local vertical cracks defined above has potentially propagated a different amount through the surface layer because of the fact that the material properties of the pavement vary spatially throughout the section. This spatial distribution of crack depths is assumed to be normally distributed. The mean of the distribution is assumed to be equal to the crack depth computed from the mechanistic model described above using the material properties measured in the laboratory. The variance of the distribution is unknown, and will be included in the model as a coefficient to be estimated during the calibration efforts. The variance will be assumed to be constant across all pavement sections.

Based upon the above assumptions, a model was developed between the amount of cracking for the pavement section and the proportion of the maximum number of vertical cracks that have actually broken through the surface layer. This model has coefficients, including the variance described above, determined from the actual field performance data as part of the model calibration.

## 6

# Fatigue Cracking Model Formulation

The total number of loading cycles required to bring about fracture of a material under a given condition is a basic fatigue property, because it is the only one which is directly measurable from experimental observations. As measured experimentally, fatigue life for a given condition is a property of the individual test specimen. Unfortunately, fatigue testing (beam fatigue tests) required to measure the fatigue life from experimental observations is highly variable and time consuming, and is not conducive for use in a mixture design procedure. For this reason, regression analyses were used to determine a more simplified relationship for use in mix design and to set design criteria for fatigue.

## 6.1 Fatigue Mechanisms

The development of fatigue cracks in a so-called ductile material consists of two different mechanisms. These are crack initiation and crack propagation. If the material is homogeneous and isotropic, there is an equal tendency for microscopic cracks to form in any specific direction. After the cracks have grown to some length in the direction of maximum shear, the tensile stress at 45° to the axis takes over, and the cracks continue to propagate in the same manner as cracks in a brittle material. Although fatigue damage is qualitatively understood, quantitative information needed to separate these two mechanisms is still rather limited .

Experimental evidence indicates that the critical value of the shearing stress for fatigue failure varies somewhat with the state of stress. A more accurate criterion is given by the octahedral shear stress theory, which states that the octahedral shear stress for fatigue failure is the same for all stress states. This is one of the reasons why the octahedral shear stress was selected as a parameter in analyzing the beam fatigue tests under the SHRP A-005 contract.

**Crack Initiation.** In developing the Superpave mix design subsystem for fatigue cracking, it was assumed that the results from stress-controlled beam fatigue tests can be used to estimate the number of loading cycles for (a visible) crack initiation. The assumption is that once a visible crack has formed it takes very few additional cycles of load to drive the crack through the test specimen and cause complete failure. Thus, under a predefined condition of crack

initiation, the number of loading cycles to cause that defined condition was used to investigate those parameters that were most closely related to crack initiation.

**Crack Propagation.** Cracks are sometimes started, but fail to propagate. An important factor here is the stress gradient or stress intensity. Cracks start in regions of high stress and if they grow in directions of decreasing stress, their growth will tend to slow down. Experimental evidence suggests that fatigue life in reversed bending is greater than an alternating simple tension and compression. Cracks also propagate at different speeds in different mixtures and under different conditions. Experiments have been performed in which crack length was measured as a function of the number of loading cycles, to determine the fracture characteristics of a material. In developing this part of the fatigue model for the Superpave mix design procedure, it was assumed that the rate of crack growth is related to the fracture energy and viscoelastic properties of the material.

## 6.2 Cumulative Damage Theory

The order in which stress levels are applied has important effects on the progress of fatigue damage. For example, a visible crack that was started under high stress levels will not propagate very rapidly under subsequent low stress levels. On the other hand, micro-cracks left by a previous low stress levels might propagate very rapidly under subsequent high stress levels. At the same time, local strain-hardening at the tip of the crack may have important bearing on how the material will behave under subsequent higher and lower stress levels.

All of these variations tend to average out if stress levels are applied in random order. For pavements, many important loading spectrums are applied in random order. Thus, it is reasonable to assume that the variations do average out, and it is on this basis that the cumulative-damage theory was developed.

According to the cumulative damage theory, each series of stress cycles account for a certain fraction of the total damage ( $D$ ), and when these fractions add up to unity, failure occurs. The fraction of the total damage done by one series of cycles at a particular stress level is given by the ratio of the number of cycles actually endured at that level to the fatigue life at the same level. This ratio is sometimes referred to as a cycle ratio, which is:

$$D_i = n_i/N_i \quad (6.1)$$

Where:  $n_i$  = actual number of load repetitions for stress level  $i$ .  
 $N_i$  = fatigue life of the material for stress level.



## 6.3 Modelling Approach

### 6.3.1 Regression Equations.

In pavement design, there have been various fatigue equations generated by different agencies to describe the number of cycles to failure for an initial strain and/or stress. One of the more common types of equations that have been used in both mix and structural design is given below:

$$N_f = k_1 (\epsilon_t)^{-k_2} \quad (6.2)$$

where:  $N_f$  = the number of load applications to reach the defined "failure" condition,  
 $\epsilon_t$  = the tensile strain induced at a critical spot in the pavement, usually the bottom of the bituminous surface layer,  
 $k_1, k_2$  = fatigue constant and coefficient developed from regression analyses.

The approach described above only looks at the externals of the fatigue process rather than looking in detail at the stress and strain gradients that are involved in the process of crack propagation. Historically, the approach finds empirical relations for  $k_1$  and  $k_2$  in terms of the modulus (elastic or loss modulus), temperature, and/or other physical properties of the asphalt concrete mix.

A problem with this empirical approach is that it does not provide an understanding of the mechanism associated with fatigue cracking. A good indicator of this is a large variation in experimentally-determined values of  $k_1$  and  $k_2$  depending on the type of material tested, the size and shape of the sample, the method of loading, and other incidentals of the testing procedure. In fact, it is known that  $k_1$  depends upon the test mode, i.e. stress-controlled v.. strain-controlled (Monismith and others, 1974), the depth of the asphalt beam sample, the method of loading, and the sample shape.

### 6.3.2 Fracture Mechanics.

"Fracture mechanics" theory can be used to provide an understanding of the phenomenon of fatigue cracking. In summary, the fracture law that is basic to crack growth in all aging, nonlinear, viscoelastic, particle-filled composite materials can be stated as:

$$U = 1/2 E_R J_V D (\hat{t}, t_a) \quad (6.3)$$

Where:  $U$  = The tensile fracture energy of the material

$J_V$  = The J-Integral, i.e., the energy released on the propagation of the crack

$D(\hat{t}, t_a)$  = The tensile creep compliance of the mix as a function of its crack propagation time,  $\hat{t}$ , and its age,  $t_a$ .

$E_R$  = The reference tensile modulus or mix stiffness.

$t$  =  $k_2 (\alpha/a)$ ; and is the crack propagation time.

$\alpha$  = The size of the damage zone ahead of the visible crack.

$a$  = The rate of crack growth =  $dc/dN$ .

$k_2$  = A constant that depends only upon the slope of the creep compliance curve,  $m$ .

It is from this basic equation that the Paris-Erdogan law of fracture mechanics and the well-known phenomenological fatigue equation can be derived. Thus, in order to predict fracture, the creep compliance properties ( $D_o$ ,  $D_m$  and  $m$ ) must be determined along with the tensile fracture energy,  $U$ , and the size of the damage zone,  $\alpha$ , which can be determined from the tensile stress-strain curve of the mixture or from the area beneath the curve out to the maximum strain that can be carried by the mix.

Working through the basic fracture relation given above shows that in the usually assumed phenomenological fatigue relation equation 6.2 or a measured relationship, the "constants"  $k_1$  and  $k_2$  are functions of the above properties of the asphalt concrete. One simple relation emerges as:

$$k_2 = 2 [m_t(1-k_t)]^{-1} \quad (6.4)$$

Where:  $m_t$  = The slope of the tensile creep compliance curve, and

$k_t$  = The exponent of the tensile stress-strain curve.

This results in the same type of relationship as in equation 6.8 above, but because it looks in much more detail at the crack propagation process, it arrives at explicit expressions for the  $k_1$  and  $k_2$  fatigue constants. Crack propagation is modeled using the Paris and Erdogan equation:

$$\frac{dc}{dN} = A(\Delta K)^n \quad (6.5)$$

where:  $dc/dN$  = the rate of growth of the crack length with respect to the number of load cycles,

$\Delta K$  = the change at the cracked tip of the stress intensity factor, and

$A, n$  = fundamental fracture properties of the asphalt concrete mix.

Applying the linear viscoelastic fracture law developed by Schapery (1984), Lytton (1993) found that the constant  $k_1$  is dependent upon: 1) the fracture parameter  $A$ ; 2) the depth of the stabilized layer; 3) the material elastic stiffness, tensile strength, and slope of the log relaxation modulus versus log time curve; and 4) the level and sign of the residual strain that remains after the passage of each load. On the other hand, the fatigue constant  $k_2$  has been found to be inversely related to the slope of the log relaxation modulus versus log time curve. Considering the crack propagation properties of a mix, in a sense, accounts for some of the differences between laboratory beam fatigue tests and the load associated cracks that occur on the roadway. In other words, it reduces the shift factor needed to match laboratory results with field performance.

## 6.4 Fatigue Cracking Model

The total number of load applications to failure, in terms of fatigue cracking, is defined or separated into a two part or phase process of crack initiation and crack growth. This is expressed mathematically by:

$$N_f = N_i + N_p \quad (7.54)$$

Where:  $N_f$  = the number of load applications to failure, where failure is defined as the point when crack length equals the layer thickness.

$N_i$  = the number of load applications to start the crack growth or crack initiation for a crack size  $C_0$ .

$N_p$  = the number of load applications to drive or propagate the crack to the surface.

### 6.4.1 Crack Initiation.

In the crack initiation phase, it is assumed that microcracks are developed and increase in size to form a visible crack with a damage zone in front of the visible crack. A microfracture model was developed by the A-005 contractor to analyze beam fatigue data. Specifically, this model was used to back calculate fracture parameters and to develop a relationship for predicting the number of load cycles to crack initiation. But first, crack initiation has to be defined to separate the number of cycles required to initiate a crack and the number to propagate that crack resulting in failure in the laboratory. Two definitions were originally considered, and both are discussed in the following paragraphs.

**Dissipated Energy.** The number of load repetitions to crack initiation in laboratory beam fatigue tests was defined to be the load cycle at which the change in dissipated energy,  $dW$ , between loading cycles  $dN$  begins to increase at an increasing rate. The rationale for this definition comes from the formulation of the microfracture model that only considers the rate

of change of dissipated energy due to the growth of microcracks,  $dW/dN$ . The reason the ratio  $dW/dN$  begins to diverge from the model is because cracks begin to develop in the beam. In this context and based on the microfracture model, the following prediction equation resulted from the use of regression analysis.

$$\begin{aligned}
 \text{Log } N_i = & b_0 + \left[ b_1 + b_2 \sigma_m + b_3 (\sigma_m^2 + 2(1 + \nu) \tau_{oct}^2) \right] E \\
 & + (b_4 \text{Log } \sigma_m + b_5 \text{Log } E) (P_{AC}) \\
 & + \left[ \frac{b_6}{E} (\sigma_m^2 + 2(1 + \nu) \tau_{oct}^2) + b_7 \text{Log } \sigma_m \right] (p_v) \\
 & + \left[ b_8 \frac{\sigma_m}{E} + b_9 \text{Log } \sigma_m \right] \frac{\sigma_m}{E}
 \end{aligned} \tag{6.7}$$

Where:  $\sigma_m$  = Mean Principal Stress, psi  
 $P_{AC}$  = Percent asphalt by weight of mix, %  
 $p_v$  = Percent air voids, %

Regression Coefficients:  $b_0 = 4.416$ ;  $b_1 = -5.421 \times 10^{-6}$ ;  
 $b_2 = 1.11 \times 10^{-7}$ ;  $b_3 = -8.518 \times 10^{-11}$ ;  $b_4 = -0.8388$ ;  
 $b_5 = 0.3148$ ;  $b_6 = 3.0893$ ;  $b_7 = -0.1148$ ;  
 $b_8 = 3.5787 \times 10^7$ ;  $b_9 = -1.244 \times 10^4$ ;  $b_{10} = 40.84$

**Stiffness Reduction.** The number of load repetitions to crack initiation was alternatively defined to be the load cycles at which there was a 50 percent reduction in the stiffness of the beam specimen. With that definition, regression analysis was used to develop a prediction equation similar, in form, to the more typical relationship found in the literature (refer to equation 6.2). The resulting prediction equation is:

$$N_i = 2.738 \times 10^5 e^{0.077VFA} (\epsilon_i)^{-3.624} (S_0^{**})^{-2.720} \tag{6.8}$$

Where:  $N_i$  = The number of load cycles in the laboratory to crack initiation which was simply defined as the condition when a 50 percent reduction in stiffness was measured or calculated.

VFA = Percent voids filled with asphalt, %

$S_0^{**}$  = Initial loss-stiffness as measured in flexure, psi

$\epsilon_t$  = Tensile strain applied to the beam specimen, or the tensile strain calculated at the bottom of the asphalt concrete layer, in./in..

Both the tensile strain and flexural loss-modulus are dependent on temperature; VFA is temperature independent. In addition, the tensile strain is dependent on or proportional to the flexural modulus, but that relationship varies with pavement structure, thickness, and environment, among other variables. The flexural modulus is related to the loss-modulus by the following equation.

$$S_o^{**} = S_o \sin \phi_s \quad (6.9)$$

Where:  $S_o$  = Initial flexural modulus, psi

$\phi_s$  = Initial phase angle between stress and strain in flexure

The flexural modulus ( $S_o$ ) has been found to be related to the shear modulus ( $G_o$ ) by the following equation:

$$G_o = \frac{S_o}{2(1+\nu)} \text{ or } G_o = 0.91 (S_o)^{0.912} \quad (6.10)$$

and

$$\sin \phi_G = 0.960 (\sin \phi_s)^{1.105} \quad (6.11)$$

Where:  $\phi_G$  = Phase angle between stress and strain in shear

**Summary.** Both alternative procedures to define or estimate the number of loading cycles to crack initiation have advantages and disadvantages as to their use in the fatigue cracking model. The SHRP A-005 contractor selected the use of the dissipated energy equation for the definition incorporated into the performance model (equation 6.7), because the definition was more compatible with the use of the fracture mechanics concept regarding crack propagation.

#### 6.4.2 Healing.

Typically, laboratory measured and field derived fatigue constants are significantly different. These differences have been attributed to the "healing" that can take place in the pavements that does not occur in laboratory fatigue tests. To account for the differences between laboratory and field conditions, predictions of fatigue life from equation 7.56 are usually adjusted through application of "shift factors". These shift factors (or sometimes referred to as calibration factors) are determined by calibration of the fatigue cracking

equation to field observations.

Pavement fatigue life is significantly influenced by the healing of microcracks between load applications and the residual stresses that build up in the pavement due to accumulation of plastic deformation. From these considerations, Tseng and Lytton (1986) developed an expression for a shift factor that is the product of a correction factor due to residual stresses and a correction factor due to healing. This equation for the shift factor was developed from laboratory healing test results and from AASHO Road Test Data. The shift factor was found to be a function of the residual stress, the fatigue constant  $k_2$ , the slope of the log relaxation modulus curve, the rest period between maximum loads, and the number of rest periods.

Here, a similar shift factor equation is used to adjust the crack initiation part of the fatigue cracking model to account for the healing that occurs between subsequent traffic loadings. The generalized form for this shift factor equation is given below:

$$N_i (\text{Roadway}) = N_i (\text{Laboratory}) * \alpha_h \quad (6.12)$$

where:  $\alpha_h$  = the shift factor, which is defined from the calibration of the model

$$\alpha_h = 1 + g_5 t_h^{g_6} \quad (6.12a)$$

$$\alpha_h = 1 + 0.049 t_h^{0.463} \quad (6.12b)$$

$t_h$  = The length of the rest period between successive load applications, seconds

$$t_h = \frac{86,400}{DTN} \quad (6.12c)$$

DTN = Daily traffic number or average daily traffic

$g_5, g_6$  = Two constants derived from calibration of the model

### 6.4.3 Crack Propagation.

Crack propagation is defined using the fracture mechanics law and the Paris-Erdogan equation form, as discussed above. The following generalized equation is used to calculate the number of load cycles to drive the crack to the surface:

$$N_p = \frac{1}{A} \int_{c_o}^h \frac{dc}{(\Delta k_{II})^n} \quad (6.13)$$

Where:  $c_o$  = Initial crack length, which is assumed to be 0.33 inches for all conditions, inches

$h$  = layer thickness, inches

$k_{II}$  = Stress intensity factor in shear

$A, n$  = Material fracture properties

The material fracture properties or parameters are being estimated using relationships that have been previously determined from other studies. The generalized forms are shown below:

$$n = g_o + \frac{g_1}{m} \quad (6.14)$$

and

$$\log A = \log g_2 + \frac{g_3}{m} \log d_1 + g_4 \log \sigma_t \quad (6.15)$$

with

$$D(t) = d_o + d_1 t^m \quad (6.16)$$

where:  $D(t)$  = creep compliance as a function of time

$d_o, d_1, m$  = parameters in the power law of the creep compliance equation, which are derived from the Superpave frequency sweep at constant height test (converting from the frequency domain to the time domain).

$t$  = time, seconds

$\sigma_t$  = tensile strength of the mix, psi

$g_0$  to  $g_4$  = five constants derived from calibration of the model

#### 6.4.4 Cracking Amount

The cracked area is evaluated by using a similar approach to the one presented by Rauhut and others (1976). The pavement geometry and material properties ( $E_{AC}$ ,  $E_B$ , ...,  $A$ ,  $n$ ) are treated stochastically, and the damage caused to the pavement is calculated by using Miner's law:

$$D_j = \sum_{k=1}^j \left( \frac{n_k}{N_{fk}} \right) \quad (6.17)$$

where:  $D_j$  = damage index after  $j$  period,

$n_k$  = actual number of load repetitions during period of time  $k$ ,

$N_{fk}$  = number of load application to failure at  $j$  period.

In the above equation, the  $N_{fk}$  is expressed as :

$$N_{fk} = N_{ik} + N_{pk} \quad (7.66)$$

where:  $N_{ik}$  = number of load repetitions that will cause crack initiation at  $j$  period, and

$N_{pk}$  = number of load repetitions that will cause crack propagation to the surface at period  $j$ .

The value of the damage index  $D_j$  is further assumed to be a normally distributed variable with a mean and variance. The stochastic expression for the mean and variance of  $D_j$  are obtained by using Cornell's first order moment theory. Following these assumptions, and for each  $D_j$  mean and variance, the probability  $F(1)$  that the variable  $D_j$  reaches the value of one (or a pavement crack) is computed and used to evaluate the cracked area by using the following expression:

$$c = 1000 [1 - F(1)] \quad (6.19)$$

where  $c$  is the expected cracked area ( $\text{ft}^2/1000 \text{ ft}^2$ ).

For the sake of simplicity and in the absence of information about the variability of the material properties, it is assumed that the variance of the relative damage due to crack initiation is neglected and the variables are independent.



## Rutting Model Formulation

As stated previously, the behavior of asphalt concrete follows that of a nonlinear visco-elasto-plastic model. The time dependent part of the materials response is important and should not be neglected. However, to satisfy the microcomputer and practicality requirements, the time dependence is accounted for by using material properties corresponding to given loading and unloading times. This assumption is an oversimplification, but will provide a reasonable estimate of the actual pavement response. The stress path that prevails in a pavement under wheel loading includes stress reversal causing rotation of the principal stress direction. Cyclic loading is thought to be better modeled by the kinematic-isotropic hardening scheme which keeps track of the loading sequence. Unfortunately, such sophisticated models do not yet exist and require uncommon testing capabilities.

The approach undertaken here for characterizing permanent deformation of pavement materials is well supported by experimental evidences, at least from two major viewpoints:

- (a) the rate of permanent deformation is based on strength parameters and increases as the stress increases toward failure, and
- (b) the permanent strain versus stress curves resulting from the model have a hyperbolic shape, similar to that obtained experimentally by Barksdale (1972) and Monismith and others (1974).

Such an approach is developed by separating the permanent deformations characterization into two parts: (a) the permanent deformation at the end of the first cycle is described using elasto-plastic models, and (b) the slope of the permanent deformation accumulation as measured from laboratory tests. The choice for the elasto-plastic approach was restricted to models that follow the non-associative flow rule which are known to be more appropriate to soils than those with an associative flow rule. The Vermeer and de Brost's general plasticity model is based on the Mohr-Coulomb failure law. Specifically, the model chosen for pavement materials characterization is taken from Vermeer's work which uses a more general failure law than the Mohr-Coulomb one (Vermeer, 1982, and Tadybakhsh and Frank, 1985).

It is worth mentioning that the strength parameters involved in the model may be slightly different from those obtained in common static tests. However, they should be

similar if the test conditions, such as rate of loading, are similar in both the repetitive and the static tests.

Permanent deformation of flexible pavements can be attributed to the consolidation of each pavement component material under repetitive traffic loading, especially the heavier loads induced by multiaxial and multiwheel vehicles. The model for permanent deformation discussed here is based on the theory of plasticity and the slope of  $\log \epsilon^P$  versus  $\log N$  relationship from laboratory test results. The basic concept of this model is described in the following subsections.

## 7.1 Permanent Deformation Characterization

The model used to represent the permanent deformation characteristics of asphalt concrete and other materials under repeated loading is the linear relation between the plastic strain and the number of repetitions on a log-log scale. The permanent deformation from a loading cycle or an applied load was characterized into two basic parts:

- (1) The permanent deformation at the end of the first loading cycle, and
- (2) The slope of the permanent deformation accumulation, as measured in the laboratory.

The resilient properties are obtained from a simulated test with 0.1 sec loading and 0.9 sec unloading, and the permanent deformation is characterized by:

$$\log \epsilon^P(N) = \log \epsilon^P(N=1) + S \log N \quad (7.1)$$

Where:  $\epsilon^P(N)$  = accumulated strain at N load repetitions. The Vermeer model is used as a framework to represent  $\epsilon^P(N=1)$  as function of the state of stress in proportional loading.

N = Number of load repetitions

S = slope of the  $\log \epsilon^P(N)$  versus  $\log N$  curve.

The model uses (a) the stresses computed under one wheel of the dual wheel, along a vertical line, at the center of the elements; (b) the Vermeer model to compute the permanent strain in the first load application,  $\epsilon^P(N=1)$  in Equation 7.1; and (c) the parameter S to compute the permanent strain at any N using Equation 7.1.

In equation 7.1,  $\epsilon^P$  and S are material properties. However, they may be dependent on the state of stress and the other material properties. The model proposed by the A-005

contractor calculates  $\epsilon^P$  from the theory of plasticity using the expression:

$$\epsilon^P = d\lambda \frac{\partial g}{\partial \sigma_{zz}} \quad (7.2)$$

where  $d\lambda$  is proportional scale,  $zz$  is the vertical direction and  $g$  is the plastic potential. A detailed discussion of the plasticity theory was given in Subsection 7.3.3. The value  $S$  is assumed to be independent of the state of stress. Additionally, the SHRP A-005 contractor found that  $S$  was related and proportional to the slope of the log frequency versus log storage modulus ( $m$ ) that are obtained from the Superpave frequency sweep at constant height test results. Thus, to decrease the number of tests required for mixture characterization, the following relationship was used in the calibration studies of the rutting performance model:

$$S = g_7 m$$

where  $g_7$  is a calibration coefficient or function.

## 7.2 Calculation of Rut Depth

The rut depth in the pavement is accumulated by summing the products of the plastic strain and the corresponding sublayer thickness during the analysis period for all seasons in the sequence. It can be expressed as:

$$RD_j = \sum_{i=1}^j \Delta RD_i = \sum_{i=1}^j \sum_{k=1}^n \epsilon_{ik}^P h_k \quad (7.3)$$

where:

$\Delta RD_i$	=	rut depth in season $i$
$RD_j$	=	rut depth accumulated up to season $j$
$\epsilon_{ik}^P$	=	permanent strain during season $i$ in element $k$
$h_k$	=	thickness of element $k$

Equation 7.3 adds all permanent deformation along the vertical line under one wheel of the dual wheel. For each season  $i$ ,  $\epsilon_i^P$  is computed from:

$$\epsilon_i^P = \epsilon_i^P (at N=1) \left[ (N_{eqi} + n_i)^S - N_{eq}^S \right] \quad (7.4)$$

where:

$\epsilon_i^P (at N = 1)$	=	permanent strain for $i$ , first load repetition computed using Vermeer model
$n_i$	=	number of load repetitions during season $i$
$N_{eqi}$	=	equivalent total number of load repetitions at beginning of season $i$
$S$	=	slope of $\log \epsilon^P - \log N$ curve derived from test results

The  $N_{eq}$  is obtained for each element k from recursive use of equation 7.4 with the time hardening marching scheme as follows

Season 1

$$N_{eq} = 0$$

$$\epsilon_1^P = \epsilon_1^P (N=1) N_1^{S_1}$$

Season 2

$$N_{eq2} = [\epsilon_1^P / \epsilon_2^P (N=1)]^{1/S_2}$$

$$\epsilon_2^P = \epsilon_2^P (N=1) [(N_{eq2} + n_2)^{S_2} - N_{eq2}^{S_2}]$$

$\ell$  Season

$$N_{eq\ell} = [\epsilon_{i-1}^P / \epsilon_i^P (N=1)]^{1/S_i}$$

$$\epsilon_i^P = \epsilon_i^P (N=1) [(N_{eq\ell} + n_i)^{S_i} - N_{eq\ell}^{S_i}]$$

The equivalent total number of load repetitions at the beginning of the  $i$ th season is obtained by using the total plastic strain at the end of the  $i - 1$  season, plastic strain at the first cycle of loading for the  $i$ th season, and slope of  $\log \epsilon^P$  versus  $\log N$  curve for the  $i$ th season. It can be expressed by the following equation:

$$N_{i,k} = \left( \frac{\epsilon_{i-1,k}^P}{(\epsilon_0^P)_{i,k}} \right)^{\frac{1}{S_{i,k}}} \quad (7.6)$$

Both of the above material properties ( $\epsilon^P$  and  $S$ ) are evaluated in the laboratory using the constant height repeated-load simple shear test where the slope,  $S$ , and intercept,  $\epsilon_0^P$  are obtained by fitting a line through the data of  $\log \epsilon_p$  versus  $\log N$ .

Rutting, on the other hand, is a three-dimensional phenomenon in which both vertical compression and lateral flow contribute to the total observed rutting. Because very little research has been done on lateral flow, there are no commonly accepted criteria relating to the measurable or predictable strains. Nevertheless, the A-005 Contractor extended the VESYS rut depth model (Kenis, 1977) into two dimensions by use of plasticity theory and found that the rate of change of plastic strains in all directions - vertical, horizontal, and shear - are proportional to their corresponding resilient strains. This method evaluates lateral

flow using elastic strains calculated with the finite element method.

One of the reasons that a more precise estimate of the lateral flow formulation was not included in the Superpave performance model is that none of the GPS projects selected for the validation effort included significant lateral flow. Thus, validation of those relationships and equations could not be supported with field data, and they were not used. More importantly, the A-005 contractor has found that the Superpave repeated shear test (at constant height or constant stress ratio) can adequately represent the observed vertical permanent deformation behavior of flexible pavement materials in the laboratory.

The permanent strain at the end of the first loading cycle,  $\epsilon^p(1)$  depends on both the material type and condition of the state of stress in a complex way. One can look at the first loading cycle separately from the other cycles and find that the first cycle in conventional repeated load tests is similar to the static test, at the loading rate of the cyclic loading. This observation made by McDonald and Raymond (1984) was used by Leshchinsky and Rawlings (1988) to approximate  $\epsilon^p(1)$  from static tests. It suggests that the elasto-plastic models developed for static loading tests are applicable to the first cycle of a repetitive load test.

In summary, a simple model for characterizing permanent deformation under cyclic loads includes two parts: (a) the permanent deformation at the end of the first cycle described using elasto-plastic models, and (b) the slope of the plastic deformation accumulation determined from laboratory test results. It is worth mentioning that this approach can also be used for visco-elasto-plastic materials using a quasi-elasto-plastic approximation (i.e., the  $\epsilon^p(1)$  and  $S$  are determined for the appropriate loading rate, and used in the elasto-plastic framework without the loading rate dependency).

## 8

### Accelerated Laboratory Tests For Performance Predictions

Five accelerated performance tests (APTs) needed to define the response characteristics of an asphalt concrete mix are employed in the Superpave level 2 and level 3 mix design methods. These tests are:

- Simple Shear at Constant Height Test
- Uniaxial Strain Test
- Volumetric Test
- Frequency Sweep at Constant Height Test
- Indirect Tensile Creep/Strength Test

Detailed descriptions of these tests and the procedures for their use in the Superpave mix design method are presented in SHRP reports SHRP-A-379 (Harrigan and others, 1994) and SHRP-A-407 (Cominsky, 1994). The frequency sweep at constant height test is analyzed in terms of linear viscoelasticity to obtain the dynamic shear modulus, the storage and loss modulus (real and imaginary parts) and the parameters of the power law. The simple shear at constant height, uniaxial strain and volumetric tests basically consist of one cycle of loading followed by unloading through three different stress paths. They serve to provide the resilient and permanent deformation characteristics of the material at the specific loading rates of the tests. The indirect tensile creep/strength test provides material characteristics required by the thermal cracking and fatigue cracking models.

#### 8.1 Analysis of Test Results

The test results are analyzed through the Superpave mix design software to yield: (a) dynamic modulus components and creep compliance parameters; (b) resilient parameters in terms of the  $k_1 - k_5$  model; (c) permanent deformation parameters in terms of the Vermeer model; and (d) rate of accumulation of permanent deformation. The frequency sweep at constant height test data are analyzed separately from the data from the other three tests, i.e., the volumetric, uniaxial strain and simple shear at constant height tests, which data are combined in one analysis.

- (a) Analysis of frequency sweep test. The Superpave software analyzes the test results and prints the storage and loss moduli at nine frequencies. These results are then used to evaluate the parameters of the power law, using the following equations (see Equations 8.1 through 8.3):

$$G(t) = g_o + g_1 t^m \quad (8.1)$$

$$G'(w) = g_o + g_1 \frac{\Gamma(l+m)}{w^m} \cos\left(\frac{\pi m}{2}\right) \quad (8.2)$$

$$G''(w) = g_1 \frac{\Gamma(l+m)}{w^m} \sin\left(\frac{\pi m}{2}\right) \quad (8.3)$$

where:

$G(t)$	=	creep compliance in shear
$g_o, g_1, m$	=	parameters of the creep compliance in shear
$w$	=	frequency
$G', G''$	=	storage and loss moduli
$\Gamma$	=	gamma function

The determination of the parameters of the creep compliance is made using nonlinear fitting of the results at the nine frequencies (minimizing the squared error between input and predicted values).

- (b) Analysis of volumetric, uniaxial strain and simple shear at constant height tests. Typical outputs of the tests are given in Figures 8.1 - 8.4 for volumetric, uniaxial strain and simple shear at constant height tests, respectively. It is seen that during the loading step, the deformation increases with time, keeps increasing, and then reduces after a certain period of time. It is seen in Figure 8.2, as an example, that the deformation keeps increasing during the whole period of unloading. However this later behavior is not typical, as most test results are similar to the behavior in Figures 8.3 and 8.4. During the period of rest after unloading, the deformation keeps decreasing with time toward an asymptotic value.

The residual deformation (which does not seem to recover) is an indication that a visco-plastic and/or plastic component exists. No attempt is made to evaluate the different components of the deformation. Instead, the quasi-time nonlinear elastoplasticity is assumed, i.e. the deformation under unloading is described using nonlinear elasticity and the deformation under loading is described using elastoplasticity. The material properties derived are therefore specific for the specific rates of loading and unloading.

- (c) Analysis of the Indirect Tensile Creep/Strength Tests. The Superpave software generates a master creep compliance curve. A Prony series expansion is used to model the compliance curve and the Arrhenius function is used for the shift factor - temperature relationship.



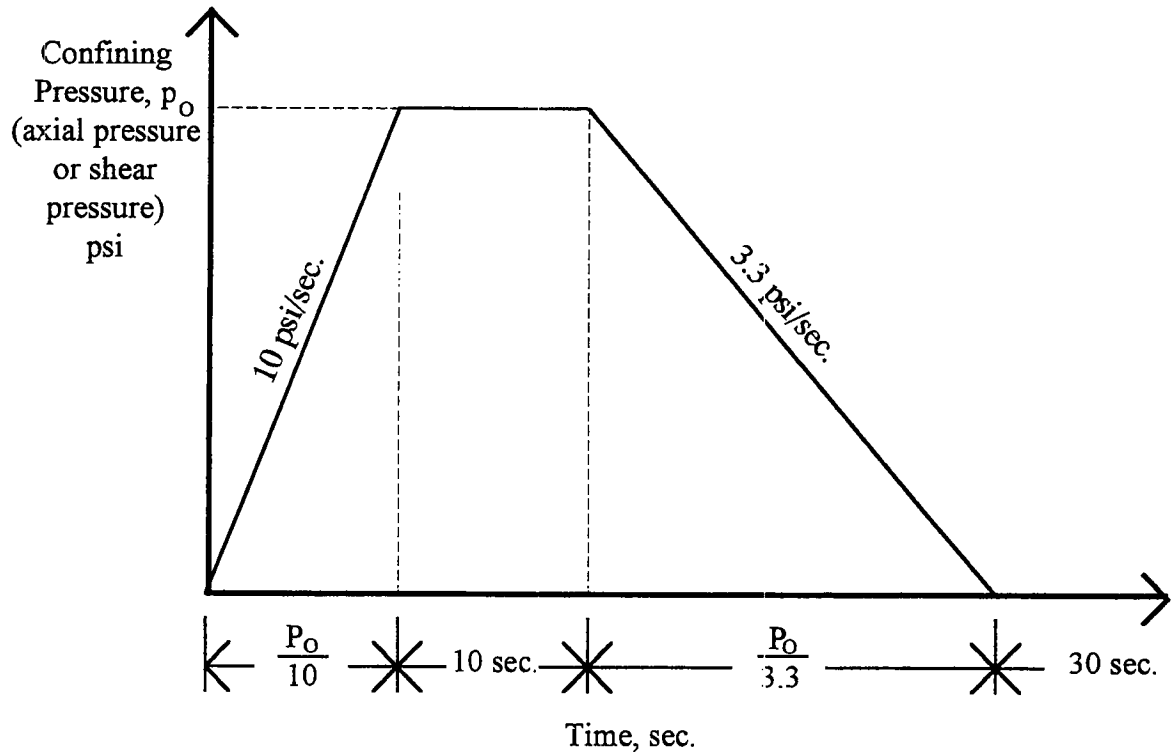


**Figure 8.1 Loading and Unloading Scheme Used in the Volumetric, Uniaxial Strain, and Constant-Height Simple Shear Tests**

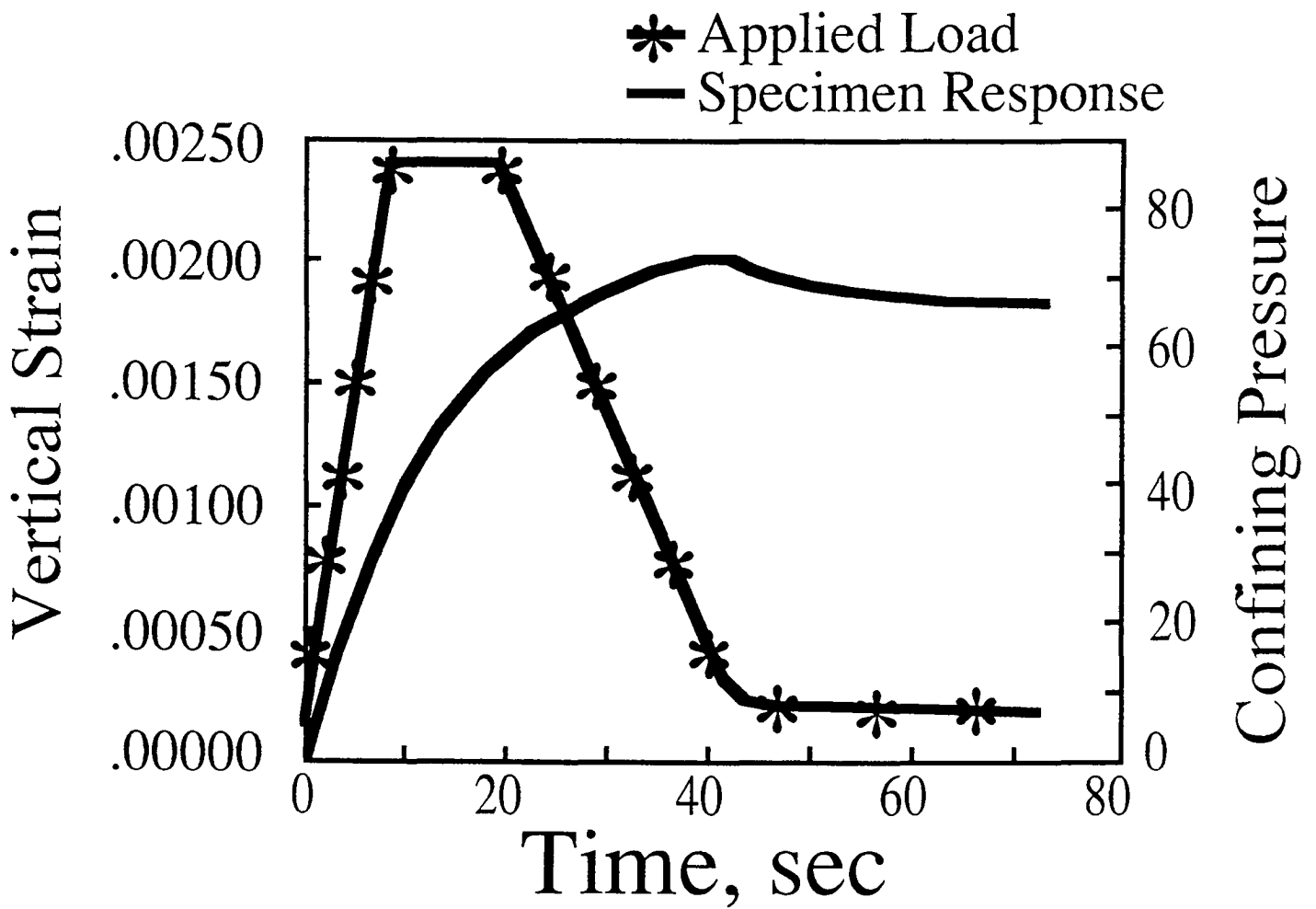


**Figure 8.2 Example of the Applied Loading (Confined Pressure) and Response Output (Vertical Strain) with Time from the Volumetric Test**

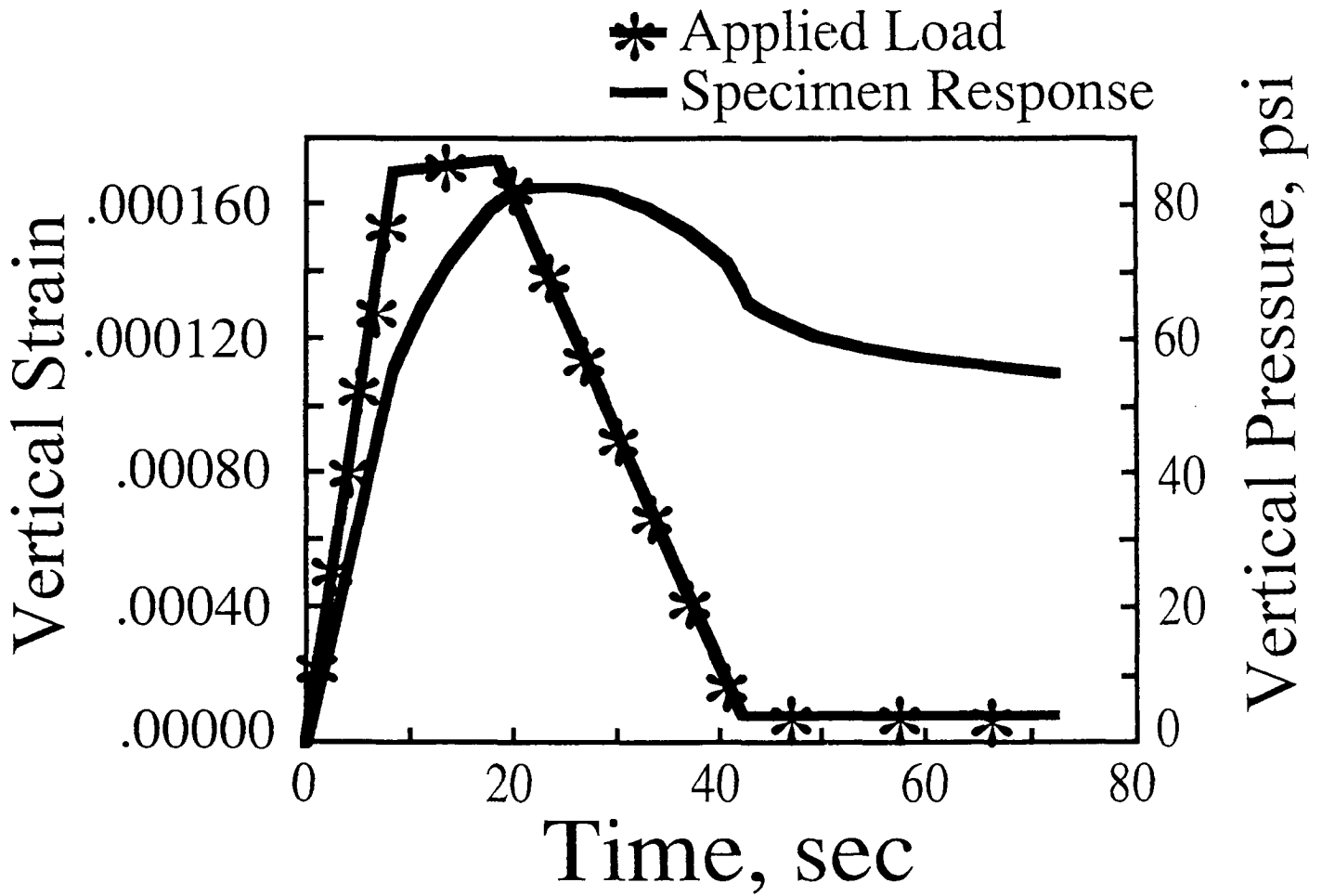
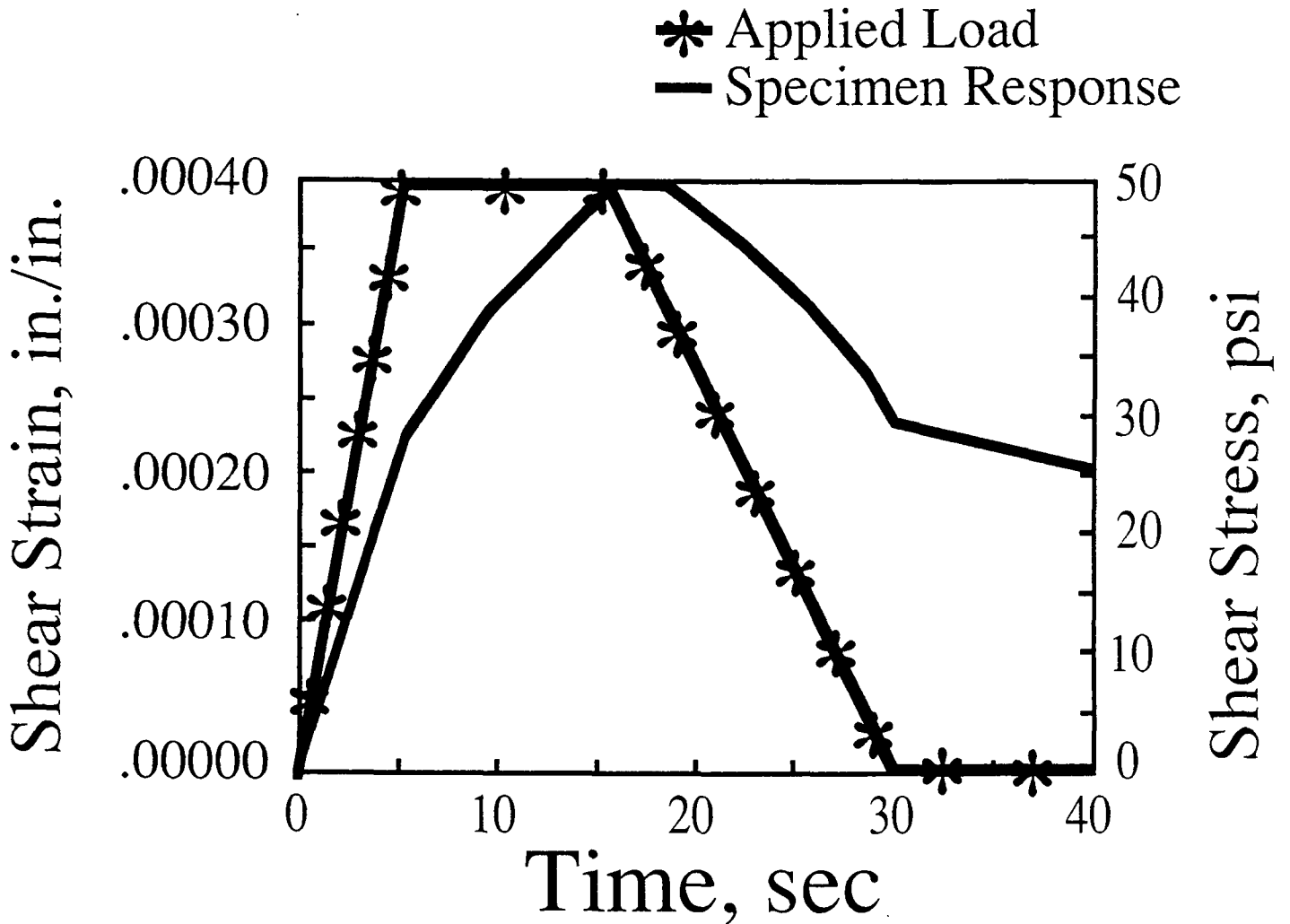


Figure 8.3 Example of the Applied Loading (Axial Load or Vertical Pressure) and Response Output (Vertical Deformation or Strain) with Time from the Uniaxial Strain Test



**Figure 8.4 Example of the Applied Loading (Shear Stress or Lateral Load) and Response Output (Shear Strain or Horizontal Deformation) with Time from the Constant-Height Simple Shear Test**

## The Superpave Pavement Performance Prediction Models

### 9.1 Aging Considerations.

In the Superpave mix design system, the process of distress prediction is significantly simplified by not considering the effects of aging. That is, the material properties do not change with time. Obviously, the modulus, strength, and other material properties do vary with time as the mixture ages and/or the binder becomes harder. However, there were only limited data collected within the SHRP program to develop a relationship that predicts this variation of mixture properties with time. Thus, the mixture properties are the same for both the crack initiation phase and crack propagation phases, as well as for the rutting predictions. Specifically, these are the shear and flexural moduli, tensile strength, phase angle, and the resilient coefficients ( $k_1$  to  $k_5$ ) used in the pavement response model.

To consider the effects of aging, it becomes important to use the critical time at which the distresses occur along the roadway. As an example, for rutting, the critical condition for measuring the mixture properties is immediately after construction (or in an unaged condition), whereas, for thermal cracking the critical condition may be after long-term aging. Thus, for fatigue cracking and rutting predictions, the test specimens are short-termed aged, while for thermal cracking predictions the test specimens can be long-term aged.

### 9.2 Non-Load Related Performance Model

A mechanics-based low temperature cracking performance model, which predicts the amount (or frequency) of low temperature cracking as a function of time, has been developed and is incorporated in the Superpave software. Inputs to the model include: fundamental properties (master creep compliance curve and failure limits as a function of temperature), pavement structure, and site-specific weather data. The calibrated model can be used to establish performance-based specification limits on the basis of material properties or parameters as determined from laboratory tensile tests. Conversely, the measured material properties can be used in the model to determine whether or not a particular mixture will meet specific low temperature cracking performance requirements. Thus, the basis is provided for a true performance-based mixture specification for low temperature cracking.

Flow diagrams of the Superpave low-temperature performance prediction model are shown in Figures 9.1 and 9.2. Figure 9.1 illustrates the interrelationships between the five major components of the model. These five components are the:

- Inputs module
- Laboratory tensile tests at low temperatures and transformation model
- Environmental effects model
- Pavement response model
- Pavement distress model

Figure 9.2 provides more detailed information for each of the model components, which are individually described in the following sections.

### *9.2.1 Inputs Module*

The input data includes the pavement structure information, the pavement material properties, and site-specific environmental data. A detailed inventory of the specific inputs in each of these three categories is as follows:

- Pavement Structure
  - Layer types: asphaltic concrete, stabilized base, or AASHTO classification for unbound granular materials and soils
  - Layer thicknesses
- Pavement material thermal properties:
  - Coefficient of thermal contraction of asphaltic concrete
  - Unit weight, thermal conductivity, heat capacity, surface emissivity factor, surface short-wave absorptivity, and maximum allowable convection coefficient of asphaltic concrete
  - Constant deep-ground temperature, freezing temperature of soil, and lower and upper limits of freezing range of soil

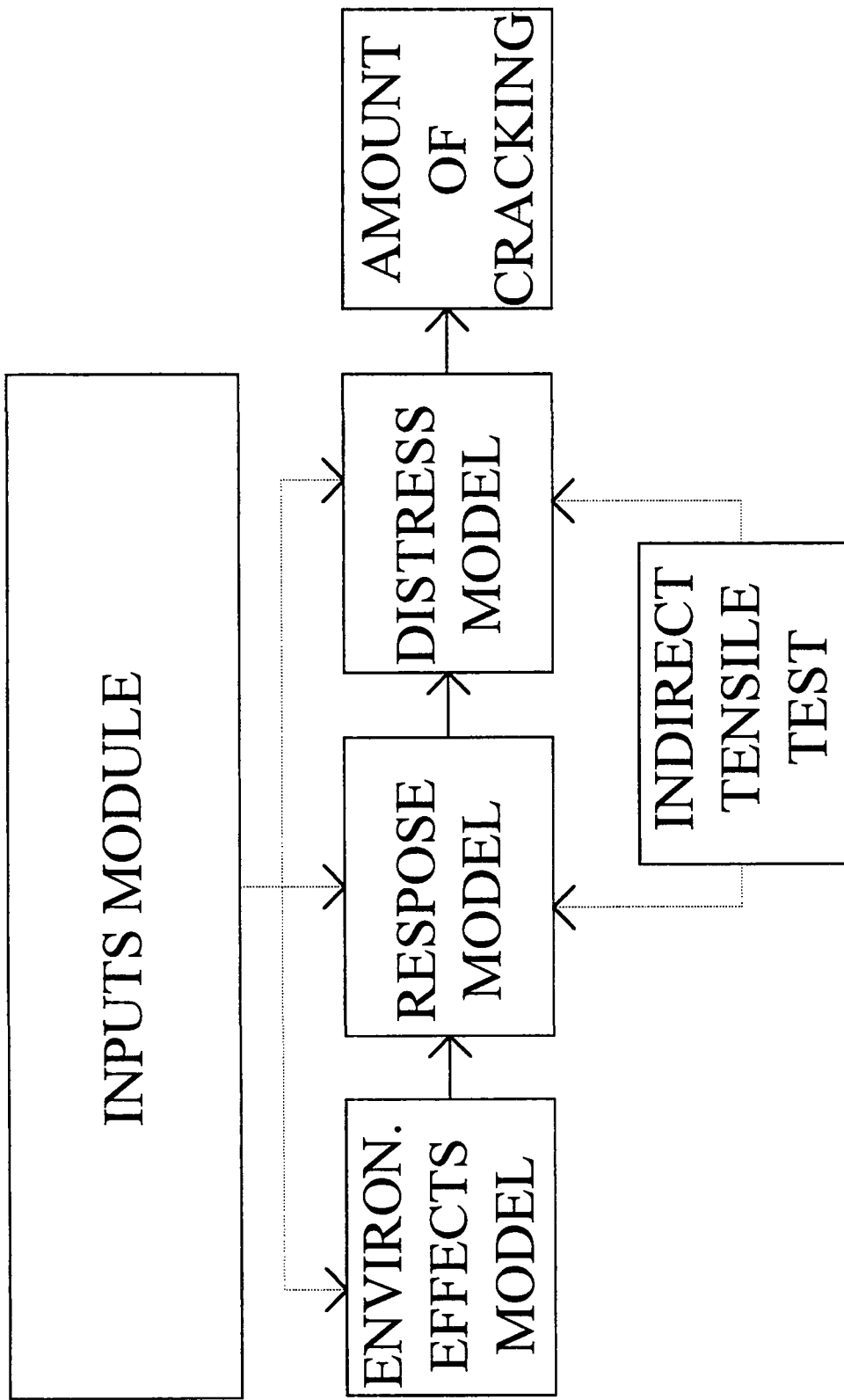


Figure 9.1 Major Components of the Low Temperature Cracking Model

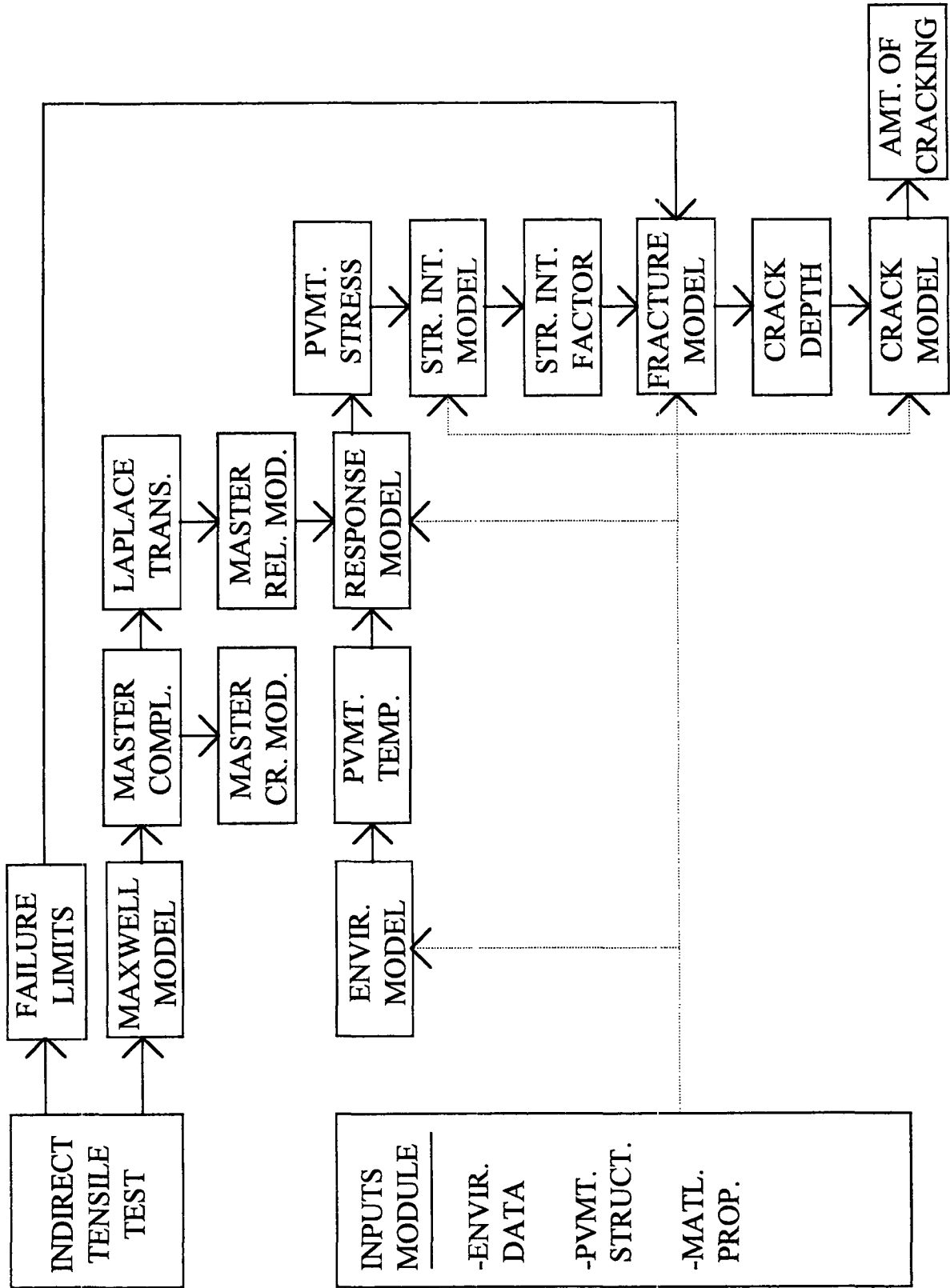


Figure 9.2 Detailed Schematic of the Low Temperature Cracking Model



- Environmental Data
  - Minimum and maximum daily air temperatures
  - Times of day when minimum and maximum air temperatures occur
  - Latitude of site
  - Average monthly wind velocity
  - Average monthly sunshine

The linear coefficient of thermal contraction for the asphalt mixture is computed using the following relationship to account for differences in the physical properties between mixes.

$$B_{MIX} = \frac{VMA * B_{AC} + V_{AGG} * B_{AGG}}{3 * V_{TOTAL}} \quad (9.1)$$

- where:
- $B_{MIX}$  = linear coefficient of thermal contraction of the asphalt mixture (1/°C)
  - $B_{AC}$  = volumetric coefficient of thermal contraction of the asphalt cement in the solid state (1/°C). Given that coefficients of thermal contractions of asphalt cement and aggregate are not measured as part of routine mixture design, an average value of volumetric coefficient of thermal contraction of  $3.45 \times 10^{-4}/^{\circ}\text{C}$  is recommended for all asphalt cements.
  - $B_{AGG}$  = volumetric coefficient of thermal contraction of the aggregate (1/°C)
  - $VMA$  = percent volume of voids in the mineral aggregate (equals percent volume of air voids plus percent volume of asphalt cement minus percent volume of absorbed asphalt cement)
  - $V_{AGG}$  = percent volume of aggregate in the mixture
  - $V_{TOTAL}$  = 100 percent

A sensitivity analysis performed using the range of contraction coefficients reported for the SHRP MRL asphalts revealed that the thermal coefficient for typical asphalt mixtures varied within in a very narrow range. The variation resulting from changes in the asphalt cement was even smaller. Similarly, the thermal contraction coefficient of a typical mixture was found to be insensitive to typical variations in reported contraction coefficients for a particular type of aggregate. One reason for this is that the coefficient of thermal contraction for the typical aggregate is about two orders of magnitude less that the contraction coefficient of asphalt cement. Therefore, it is adequate to use published values of contraction coefficients for the type of aggregate being used.

Contraction coefficients determined from this relationship appear to reasonably accurate. Coefficients determined for four mixtures produced from SHRP MRL materials, agreed well with measured values reported by most researchers in the literature, and resulted in reasonably accurate predictions of thermal stresses and fracture temperatures measured in the thermal stress restrained specimen test (TSRST).

### **9.3 Laboratory Tensile Tests and the Transformation Model**

#### *9.3.1 Tensile Tests at Low Temperatures.*

Two types of tensile tests are conducted on asphaltic concrete specimens: a short-term creep test (approximately 1000 seconds), followed by a test to failure at a constant stroke rate. The results forwarded to the model from this test are the average 1000-second creep compliance curves at three temperatures (see Figure 9.3) and the average tensile strengths at three temperatures. The average data are typically based upon tests on three replicate specimens.

#### *9.3.2 Transformation Model.*

The purpose of the transformation model is to determine the master relaxation modulus curve from the creep compliance measurements and to determine the relationship between failure strength and temperature. The transformation from the creep compliance test results to the master relaxation modulus curve is accomplished in two steps. First, the master creep compliance curve is generated from the creep compliance test results at different temperatures. A Prony series expansion is used to model the compliance curve, and an Arrhenius function is used for the shift factor-temperature relationship. Second, the master relaxation modulus curve is determined from the master creep compliance curve via Laplace transformations.

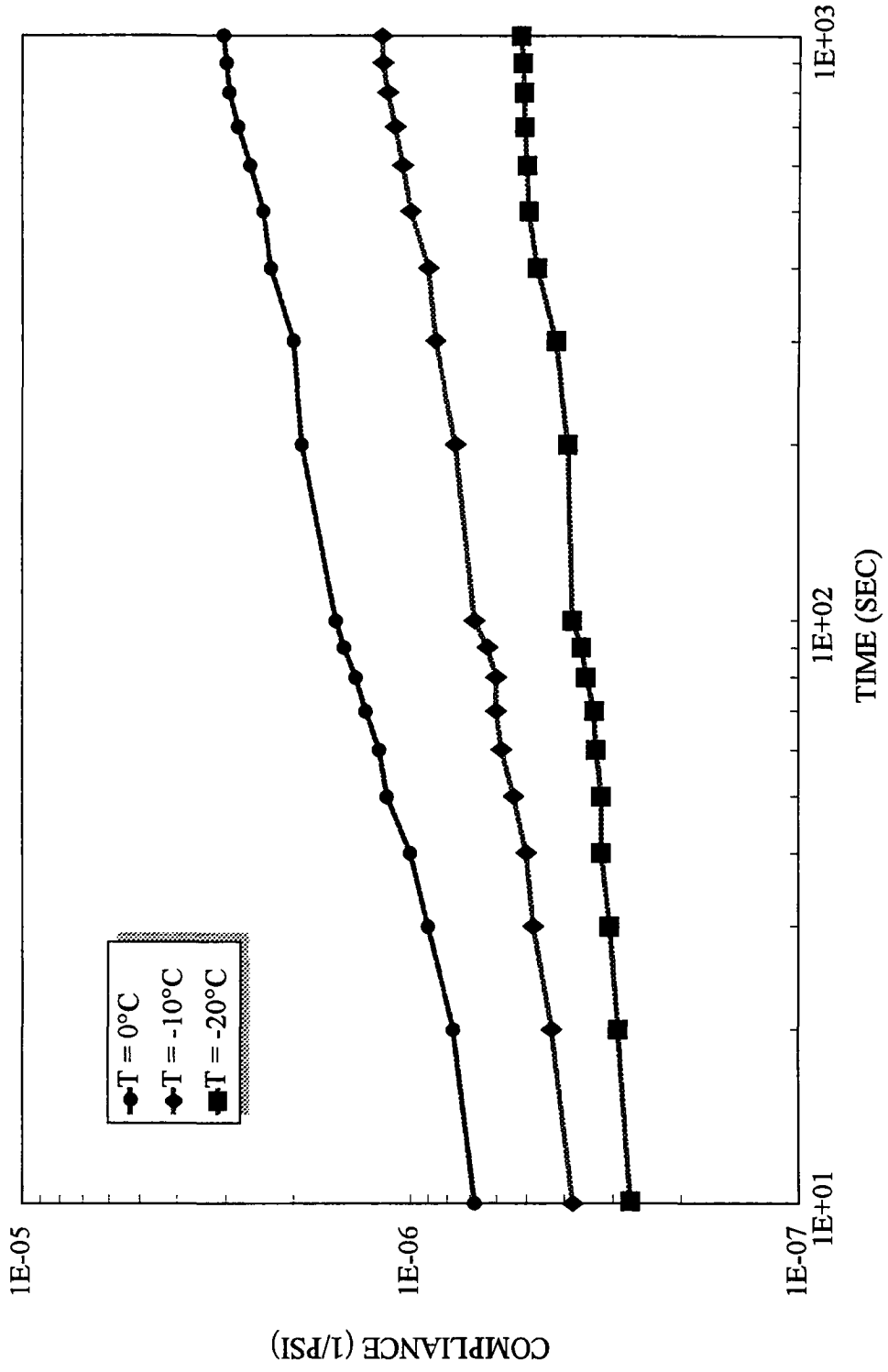


Figure 9.3 Creep Compliance Curves for PTI Section 23

Master Creep Compliance Curve. A nonlinear regression routine is used to determine the master creep compliance curve from the creep compliance curves measured at multiple temperatures. This regression is performed in three steps. First, a regression is performed to simultaneously determine the temperature shift factors ( $a_T$ ) and the parameters for the following Prony series (Maxwell model) representation of the master creep compliance curve:

$$D(\xi) = D(0) + \sum_{i=1}^N D_i(1 - e^{-\xi/\tau_i}) + \frac{\xi}{\eta_v} \quad (9.2)$$

where:

$D(\xi)$	=	creep compliance at reduced time $\xi$
$\xi$	=	reduced time = $t/a_T$
$a_T$	=	temperature shift factor
$D(0), D_i, T_i, \eta_v$	=	Prony series parameters

In essence, the regression finds the best shift factors and Prony series parameters that fit the measured data based upon a least-squares criterion. One of the test temperatures is selected as the reference temperature for the master curve. Thus, the creep compliance curve at this temperature is fixed in time ( $a_T=1$ ). The regression determines the amount of time (horizontal) shift required for the curves at the remaining temperatures to result in a smooth master curve. Each of these remaining creep compliance curves will have a shift factor ( $a_T$ ) associated with it.

In conjunction with the determination of the shift factors, the regression determines the coefficients for the Prony series. Four Maxwell elements ( $N=4$ ) have been found to be sufficient to fit the data accurately when creep compliance curves at three temperatures (-20, -10, and 0°C) are used to construct the master curve. The master creep compliance curve and the shift factors as a function of temperature for the test results previously presented in Figure 9.3 are shown in Figures 9.4 and 9.5, respectively.

The Prony series (Maxwell model) was chosen to represent the master creep compliance curve for three primary reasons:

- Experience has shown that this functional form fits the measured data extremely well (see Figure 9.4).
- The Prony series greatly simplifies the transformation of the master creep compliance curve to the master relaxation modulus curve (described in the next section).
- The Prony series greatly simplifies the solution of the viscoelastic constitutive model used to calculate pavement stresses (described in Pavement Response Model section below).

The second step in the regression routine is to fit a functional form to the shift factor versus temperature data. The following Arrhenius function is used for this functional form:

$$a_T = e^{\frac{H}{R} \left( \frac{1}{T} - \frac{1}{T_{REF}} \right)} \quad (9.3)$$

where:

$a_T$	=	shift factor for temperature $T$
$T_{REF}$	=	reference temperature for master creep compliance curve
$H$	=	activation energy
$R$	=	ideal gas constant

The result of this regression is a value for the ratio of  $H$  to  $R$ . The Arrhenius function fit of the shift factors determined from the creep compliance data in Figure 9.3 is shown in Figure 9.5.

The third step in the regression routine is to fit a second functional form to the master creep compliance information. This second functional form is the following power law:

$$D(\xi) = D_o + D_1 \xi^m \quad (9.4)$$

where  $D(\xi)$  and  $\xi$  are as defined previously, and  $D_o$ ,  $D_1$ , and  $m$  are the coefficients of the functional form. The primary purpose for fitting this functional form is to determine the parameter  $m$ . This parameter is essentially the slope of the linear portion of the master creep compliance curve on a log-log plot. It has been found to be an important parameter in distinguishing between the low temperature cracking performance of different materials, and is a direct input into the crack depth (fracture) model described below.

**Master Relaxation Modulus Curve.** The viscoelastic constitutive equation used in the pavement response model requires that the time and temperature dependent relaxation modulus of the material be known. It is common to formulate the constitutive equations in terms of relaxation modulus when the stress response to a known strain input is desired, which is the case here. However, it is also accepted and understood that creep tests on viscoelastic materials are easier to conduct than relaxation test results. Therefore, a laboratory tensile creep test was used for measuring the viscoelastic properties.

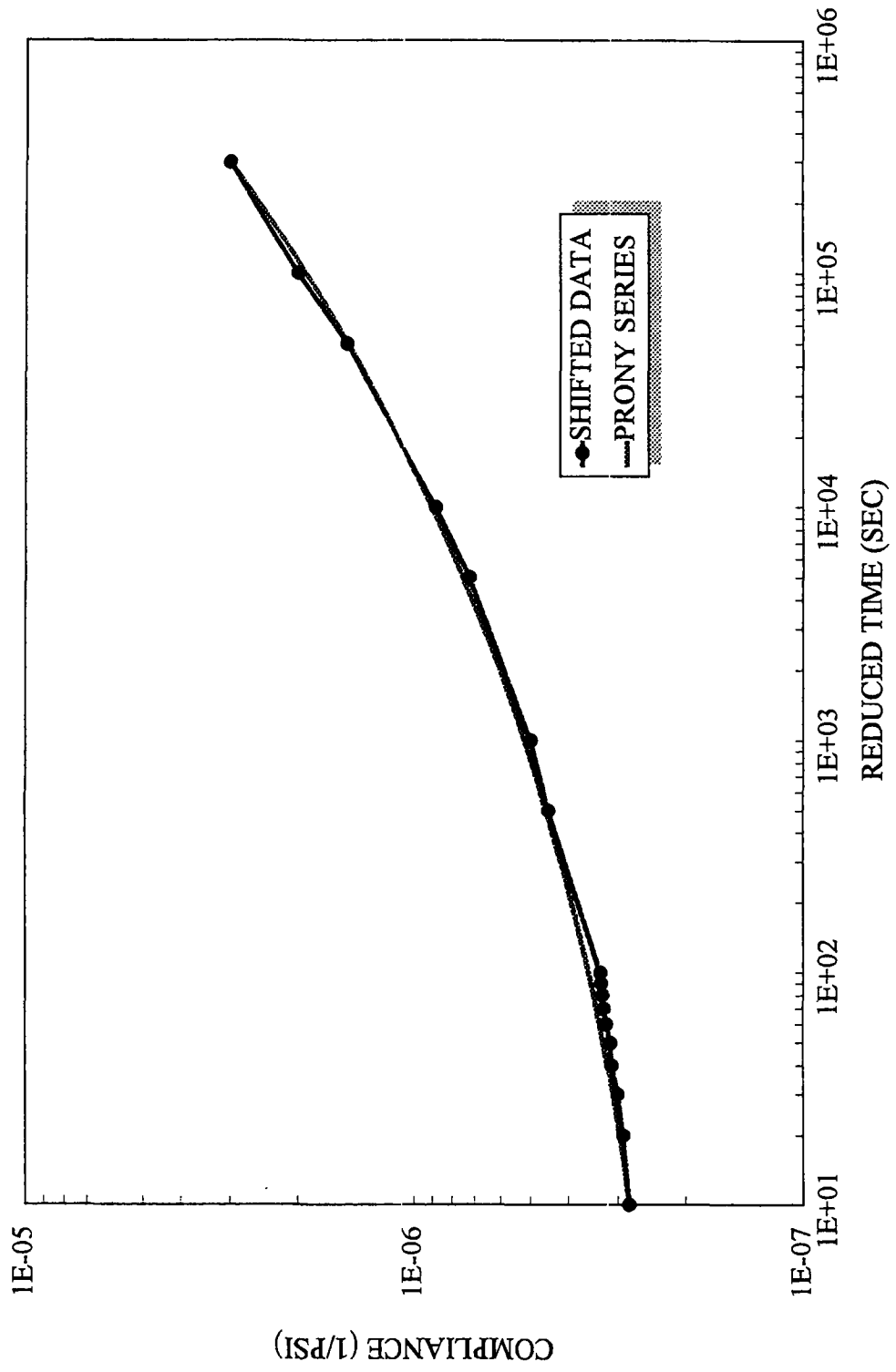


Figure 9.4. Master Creep Compliance Curve for PTI Section 23

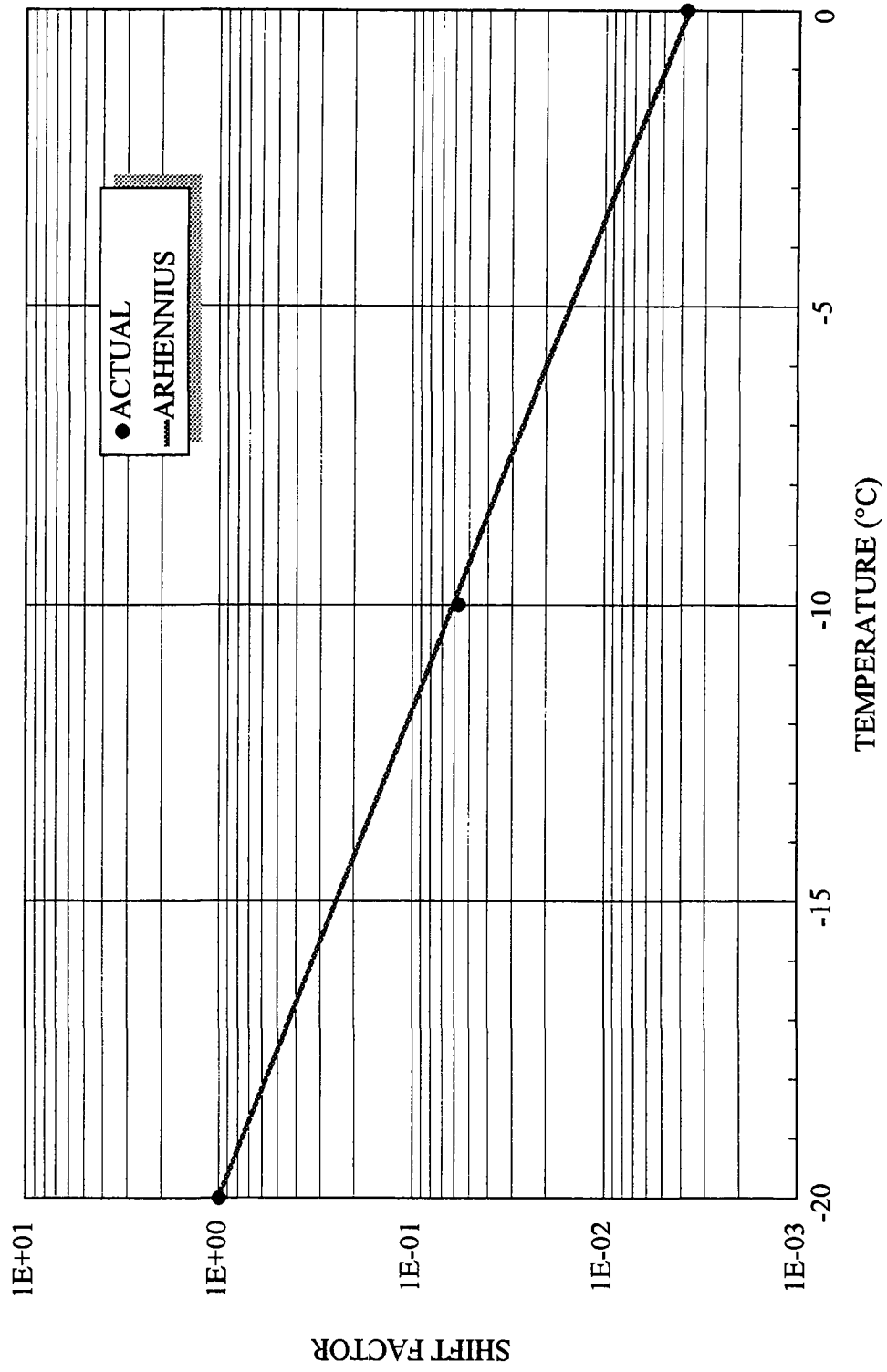


Figure 9.5 Shift Factor versus Temperature for PTI Section 23

The viscoelastic property determined from a creep test is known as the creep compliance. The creep compliance is simply the time dependent strain divided by the constant stress. However, the property required for the stress predictions is the relaxation modulus, as discussed above. Sometimes the relaxation modulus is approximated as simply the inverse of the creep compliance, which is not truly correct.

The inverse of the creep compliance is the creep modulus and not the relaxation modulus. Although under some conditions (low temperatures and short loading times with hard materials) the two moduli are approximately equal, this is generally not the case. Since the creep compliance and the true relaxation modulus are related, it is relatively simple to determine the true relaxation modulus, rather than approximate it. As previously discussed, the calculations are particularly easy if a Prony series is used to represent the master creep compliance curve.

For a viscoelastic material, the relationship between creep compliance and relaxation modulus is:

$$sL[D(t)] * sL[E(t)] = 1 \quad (9.5)$$

where:

$L[D(t)]$	=	the Laplace transformation of the creep compliance, $D(t)$
$L[E(t)]$	=	the Laplace transformation of the relaxation modulus, $E(t)$
$s$	=	the Laplace parameter
$t$	=	time (or reduced time, $\xi$ )

A computer program was developed to solve this equation for the master relaxation modulus,  $E(\xi)$ , given the master creep compliance,  $D(\xi)$ . The program essentially performs the following steps:

1. Computes the Laplace transformation of the master creep compliance curve,  $L[D(\xi)]$ , where  $D(\xi)$  is defined by the Prony series described above
2. Multiplies  $L[D(\xi)]$  by  $s^2$
3. Computes the reciprocal of  $s^2 * L[D(\xi)]$
4. Computes  $E(\xi)$ , which is the inverse Laplace transformation of the Step 3 result.  $E(\xi)$  will then have the following Prony series functional form:

where:

$E(\xi)$	=	relaxation modulus at reduced time $\xi$
$E_p \lambda_i$	=	Prony series parameters for master relaxation modulus



$$E(\xi) = \sum_{i=1}^{N+1} E_i e^{-\xi/\lambda_i} \quad (9.6)$$

curve

The transformation program has been independently verified by comparing the results to those produced by the "Maple" program, which is a mainframe symbolic algebra system that is able to perform Laplace transformations. Comparisons made between the relaxation modulus computed as described, and the creep modulus have shown that the two properties are not equivalent. Thus, it would not be accurate to approximate the relaxation modulus with the creep modulus. The master relaxation modulus curve determined from the master creep compliance curve presented in Figure 9.4 is shown in Figure 9.6.

## 9.4 Load Related Performance Models

The data from the test results is processed as follows:

- (1) Since the maximum load level may vary with the test, the times at which the various loading sequences begin are determined using the given creep time of 10 seconds, the rest period after unloading of 10 or 30 seconds, and loading rates of 10 or 3 psi/s.
- (2) The time at which the loading (at constant rate) sequence ends is determined more specifically. First the minimum of the data values of the load during the period where the load is kept constant is determined. Then the data is scanned from the beginning and the new time at which the loading (at constant rate) is the smallest time at which the load reaches a value equal to the minimum determined above times 0.98.

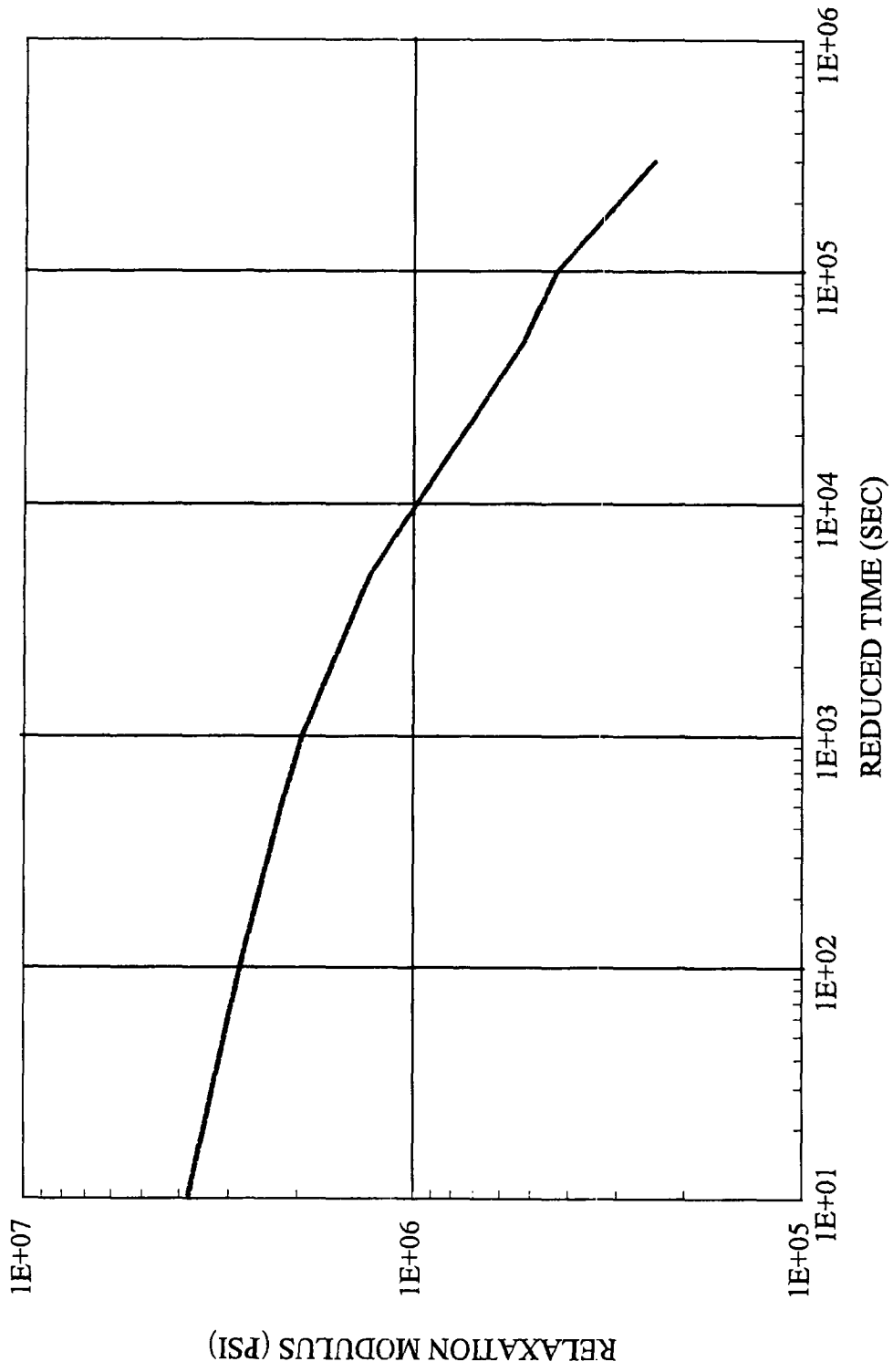


Figure 9.6 Master Relaxation Modulus Curve for PTI Section 23

- (3) The time at which the unloading (at constant rate) sequence ends is determined in a manner similar to (2) above.
- (4) The loading sequence is subdivided into 10 equally spaced intervals and averages of 3 readings of the load and of the deformations are calculated.
- (5) Because of visco-elasto-plastic nature of asphalt concrete, the response during unloading is affected by previous loading/unloading sequences. Therefore an extrapolation of the response during the creep period (at which the load is kept constant) is required. After several trials, the following equation is used to fit the data in the last 8 seconds of the 10 second creep:

$$\epsilon(t) = a_0 + a_1(t - a_2)^{a_3}$$

where:

$\epsilon(t)$	=	material deformation response
$t$	=	time from beginning of test
$a_0 - a_3$	=	fitting parameters

- (6) The unloading response is calculated using the data acquired during unloading, and the material response (if no unloading was taking place) is predicted using Equation 9.5. In other words, the response given by Equation 9.6 is the base or reference of the unloading sequence. As in (4) above, the unloading sequence is subdivided into 10 equally spaced intervals and averages of 3 readings of the load and the deformations are determined.

## References

Barksdale, R.D. (1972), "Laboratory Evaluation of Rutting in Base Course Materials," Proceedings of the 3rd International Conference on the Structural Design of Asphalt Pavements, University of Michigan, pp. 161-174.

Cominsky, R.J. et al. (1994), "The Superpave Mix Design Manual for New Construction and Overlays," Strategic Highway Research Program Report SHRP-A-407, Washington.

Duncan, J.M. and Seed, A.M. (1986), "Compaction-Induced Earth Pressures and K-Conditions," ASCE Journal of Geotechnical Engineering, Volume 112, No. 1, pp. 1-22.

Hanson, J.B. (1965), "Some Stress-Strain Relationships for Soils," Proceedings of the 6th International Conference on Soil Mechanics and Foundation Engineering, Volume 1, pp. 231-234, Montreal.

Harrigan, E.T. et al. (1994), "The Superpave Mix Design System Manual of Specifications, Test Methods, and Practices," Strategic Highway Research Program Report SHRP-A-379, Washington.

Houlsby, G.T. (1986), "A General Failure Criterion for Frictional and Cohesive Materials," Soils and Foundations, Japanese Society of Soil Mechanics and Foundation Engineering, Volume 26, No. 2, pp. 97-101.

Kenis, W.J. (1977), Predictive Design Procedures, VESYS Users Manual -- A Design Method for Flexible Pavements Using the VESYS Structural Subsystem," Proceedings of the 4th International Conference on Structural Design of Pavements, University of Michigan, pp. 101-138.

Lade, P.V. and Nelson, R.D. (1987), "Modelling the Elastic Behavior of Granular Materials," International Journal for Numerical and Analytical Methods in Geomechanics, Volume II, pp. 521-542.

Leshchinsky, D. and Rawlings, D.L. (1988), "Stress Path and Permanent Deformations in Sand Subjected to Repeated Load," ASTM Geotechnical Testing Journal, March 1988, pp. 36-43.

Lytton, R.L., Pufahl, D.E., Michalak, C.H., Liang, H.S., and Dempsey, B.J. (1990), "An Integrated Model of the Climatic Effects on Pavements," Federal Highway Administration Report FHWA-RD-90-033.

Lytton, R.L., Uzan, J., Fernando, E.G., Roque, R., Hiltunen, D. and Stoffels, S.M. (1993), "Development and Validation of Performance Prediction Models and Specifications for Asphalt Binders and Paving Mixes," Strategic Highway Research Program Report SHRP-A-357, Washington.

Matsuoka, H. and Nakai, T. (1985), "Relationship among Tresca, Mises, Mohr-Coulomb and Matsuoka-Nakai Failure Criteria," Soils and Foundations, Japanese Society of Soil Mechanics and Foundation Engineering, Volume 25, No. 4, pp. 123-128.

McDonald, L.M. and Raymond, G.P. (1984), "Repetitive Load Testing: Reversal or Rotation," Canadian Geotechnical Journal, Volume 21, pp. 456-474.

Molenaar, A.A.A. (1983), "Structural Performance and Design of Flexible Road Constructions and Asphalt Concrete Overlays," Delft University of Technology.

Monismith, C.L., Ogawa, N., and Freeme, C.R. (1974), "Pavement Deformation Characteristics of Subgrade Soils due to Repeated Loading," Transportation Research Record 537, Transportation Research Board, Washington, pp. 1-17.

Owen, D.J.R. and Hinton, E. (1980), "Finite Elements in Plasticity: Theory and Practice," Pineridge Press Limited, Swansea, United Kingdom.

Rauhut, J.B., O'Quin, J.C. and Hudson, W.R. (1976), "Sensitivity Analysis of FHWA Structural Model VESYS II, Volume I: Preparatory Studies and Volume II: Sensitivity Analysis," Federal Highway Administration Reports FHWA-RD-76-23 and FHWA-RD-76-24.

Schapery, R.A. (1984), "Correspondence Principles and a Generalized J Integral for Large Deformation and Fracture Analysis of Viscoelastic Media," International Journal of Fracture, Volume 25, pp. 195-223.

Schapery, R.A. (1986), "Time-Dependent Fracture: Continuation Aspects of Crack Growth," Encyclopedia of Materials Science and Engineering, M.B. Bever (editor), Pergamon Press Inc., Elmsford, NY, pp. 5043-5053.

Seed, A.M. and Duncan, J.M. (1986), "FE Analysis Compaction Induced Distresses and Deformations," ASCE Journal of Geotechnical Engineering, Volume 112, No. 1, pp 23-43.

Tadjbakhsh, S. and Frank, R. (1985), "Etude par la méthode des éléments finis du comportement élastoplastique des sols dilatants, Application aux pieux sous charge axiale," Rapport de recherche LPC No. 135, LCPC, France, p. 140.

Tseng, K.H. and Lytton, R.L. (1986), "Prediction of Permanent Deformation in Flexible Pavement Materials," ASTM Symposium on the Implication of Aggregates in the Design, Construction and Performance of Flexible Pavements, New Orleans.

Uzan, J., Zollinger, D.G., and Lytton, R.L. (1990), "The Texas Flexible Pavement System (TFPS)," Volume II, Federal Highway Administration Report FHWA/TX-91/455-I, Austin, Texas.

Vermeer, P.A. (1982), "A Five-Constant Model Unifying Well Established Concepts," International Workshop on Constitutive Relations for Soils, Grenoble, France, 6-8 September, pp. 175-197.

Vermeer, P.A. and de Brost, R. (1984), "Non-Associated Plasticity for Soils, Concrete, and Rock," HERON Journal, Delft University of Technology, Delft, The Netherlands, Volume 29, No. 3, pp. 1-64.

Witczak, M.W. and Uzan, J. (1988), "The Universal Airport Pavement Design System - Report I of IV: Granular Materials Characterization," The University of Maryland, Department of Civil Engineering, College Park, Maryland.

## **Asphalt Advisory Committee**

Thomas D. Moreland, *chairman*  
*Moreland Altobelli Associates, Inc.*

Gale C. Page, *vice chairman*  
*Florida Department of Transportation*

Peter A. Bellin  
*Niedersachsisches Landesamt  
für Strassenbau*

Dale Decker  
*National Asphalt Paving Association*

Joseph L. Goodrich  
*Chevron Research Company*

Eric Harm  
*Illinois Department of Transportation*

Charles Hughes  
*Virginia Highway & Transportation Research Council*

Robert G. Jenkins  
*University of Cincinnati*

Anthony J. Kriech  
*Heritage Group Company*

Richard Langlois  
*Universite Laval*

Richard C. Meininger  
*National Aggregates Association*

Nicholas Nahas  
*EXXON Chemical Co.*

Charles F. Potts  
*APAC, Inc.*

Ron Reese  
*California Department of Transportation*

Donald E. Shaw  
*Georgia-Pacific Corporation*

Scott Shuler  
*The Asphalt Institute*

Harold E. Smith  
*City of Des Moines*

Thomas J. Snyder  
*Marathon Oil Company*

Richard H. Sullivan  
*Minnesota Department of Transportation*

A. Haleem Tahir  
*American Association of State Highway and  
Transportation Officials*

Jack Telford  
*Oklahoma Department of Transportation*

George West  
*Shell Oil Company*

## **Liaisons**

Avery D. Adcock  
*United States Air Force*

Ted Ferragut  
*Federal Highway Administration*

Donald G. Fohs  
*Federal Highway Administration*

Fredrick D. Hejl  
*Transportation Research Board*

Aston McLaughlin  
*Federal Aviation Administration*

Bill Weseman  
*Federal Highway Administration*

## **Expert Task Group**

Dave Allen  
*University of Kentucky*

Daniel W. Dearasaugh, Jr.  
*Transportation Research Board*

Ervin Dukatz  
*Vulcan Materials*

Charles Manzione  
*United States Air Force*

Bill Maupin, Jr.  
*Virginia Transportation Research Council*

Richard May  
*The Asphalt Institute*

Roy McQueen  
*Rajan-McQueen and Associates*

James A. Sherwood  
*Federal Highway Administration*

George Way  
*Arizona Department of Transportation*